AN ABSTRACT OF THE THESIS OF

SURYYA KANTA SARMAH (Name) for the Ph. D. (Degree) in GEOPHYSICS (Major)

Date thesis is presented 19 August 1966

Title ATTENUATION OF COMPRESSIONAL WAVES IN THE EARTH'S MANTLE

Abstract approved Redacted for Privacy (Major professor)

Fourier transformed amplitudes of the compressional waves recorded between 9° and 91° (about 1000 to 10,000 km) epicentral distance from Gnome, Shoal, Haymaker, and Bilby underground nuclear explosions have been compared with Fourier transformed amplitudes of P waves measured at distances between 9.0 and 13.0 km from the explosions. Using a formula of the type

$$A = \epsilon A_0 F(\xi) e^{-\frac{\pi f r}{QV}}$$

apparent Qs have been computed for frequency ranges of 0.5 to 1.0 cps and 0.7 to 1.0 cps at the various epicentral distances. The geometrical spreading factor $F(\xi)$ and interface loss parameter ϵ drop out of the computations when assumed to be frequency independent in the narrow frequency pass-bands considered.

The computed apparent Q values indicate that the mantle is inhomogeneous with respect to the absorption of seismic energy.

Relatively low Q (high absorption) regions are centered around 25°, 42° and 74° and high Q (low absorption) regions are centered around 20°, 31°, 71°, and 78° epicentral distances. These are superimposed on a gradually increasing Q with epicentral distance trend. The average apparent Q value for the upper mantle is found to be 286 ± 38. The highest Q value of this study occurs between 78° and 80° epicentral distance where it is greater than 3000.

The high and low Q values obtained in this investigation are of the same order of magnitude as those reported by other investigators from body wave studies and the general variation of the absorption properties with depth agrees reasonably well with those obtained from surface wave studies. The depth of great increase in electrical conductivity and the observed maximum depth of earthquake foci both agree roughly with a region of large increase in Q in the upper mantle. A relatively high absorption zone is found to occur below this depth.

ATTENUATION OF COMPRESSIONAL WAVES IN THE EARTH'S MANTLE

by

SURYYA KANTA SARMAH

A THESIS

submitted to

OREGON STATE UNIVERSITY

in partial fulfillment of
the requirements for the
degree of

DOCTOR OF PHILOSOPHY

June 1967

APPROVED:

Redacted for Privacy

Professor of Geophysics
In Charge of Major

Redacted for Privacy

Chairman of Department of Oceanography

Redacted for Privacy

Dean of Graduate School

Date thesis is presented 19 August 1966

Typed by Gwendolyn Hansen

ACKNOWLEDGMENT

This research was performed under the direction of Dr. Joseph W. Berg, Jr., Professor of Geophysics at Oregon State University. The author is grateful to Dr. Berg for his assistance in all phases of this work, particularly for his many helpful suggestions and discussions in the analysis of data and in writing this thesis.

Appreciation is extended to the U. S. Coast and Geodetic Survey, Teledyne Industries, Dominion Observatory of Canada, and Dr. W. Stauder, S. J., of St. Louis University for supplying the seismograms used in this research.

Appreciation is also extended to Mrs. Susan Borden, Department of Oceanography and Mr. Walter M. Pawley for their help in computer programming.

This research was supported by the Air Force Office of Scientific Research under Grant AF - AFOSR - 49(638)-1403 as part of the Vela Uniform Program directed by the Advance Research Project Agency of the Department of Defense.

TABLE OF CONTENTS

LIST OF TABLES

LIST OF APPENDIX TABLES

LIST OF FIGURES

LIST OF APPENDIX FIGURES

ATTENUATION OF COMPRESSIONAL WAVES IN THE EARTH'S MANTLE

INTRODUCTION

Objective

In a perfectly elastic solid, incremental strain at any point is a linear function of the stress applied at that point. Equations based on stress-strain relationships allow prediction of amplitudes, among other things, for waves propagating in an elastic medium. The amplitudes for such waves are affected by attenuation losses which are (1) geometrical spreading and (2) scattering and mode conversions when the medium is inhomogeneous.

Theoretically, compressional or other types of waves will have none of their energy absorbed by a perfectly elastic medium while propagating through it. However, laboratory and field observations show that there is always some absorption of wave energy by earth materials because of imperfect elasticity. This loss of amplitude or energy is the third type of attenuation, (3) the absorptive attenuation, and will be the topic of discussion in this thesis.

The main tool for investigating the earth's interior is seismic waves. Studying the compressional waves recorded at different epicentral distances on the surface of the earth gives information

about the elastic properties of the interior. The manifestation of seismic wave attenuation in the interior of the earth is the diminution of amplitude with distance. Because of the complications introduced by the poorly defined sources and local geology both at the source and receiving stations, it has been difficult to obtain amplitude information suitable for attenuation studies of compressional waves. Special difficulties in studying such waves in the inhomogenous earth are mode conversions at the interfaces, scattering and complicated geometrical spreading losses.

Underground nuclear explosions have given an unusual opportunity for studying the attenuation of compressional seismic waves which have travelled through the earth. Seismic waves from such explosions are recorded from very close to the explosion point to teleseismic distances with calibrated instruments. As a result, the sources have been well documented in many instances, and comparison of known source amplitude data with those measured at various distances from the source becomes feasible. It is the object of this thesis to determine the amplitude losses concerned with absorptive attenuation by making such a comparison using data from several nuclear explosions.

Theory of Absorptive Attenuation

There is no general agreement as to the best way of representing absorptive attenuation of seismic waves. However, various investigators have used a dimensionless quantity Q that is the quality factor or specific dissipation function $1/Q$. This Q has been introduced into mechanical problems from an analogy with electrical circuit theory. The steady state current in an L, R, C circuit is given by the differential equation (60):

$$L\frac{di}{dt} + Ri + \frac{1}{C}\int idt = 0. \qquad (1)$$

Then Q is generally defined as the quantity

(1) $$Q = \frac{2\pi \text{ (energy stored in the circuit)}}{\text{energy loss per period}} \qquad (2)$$

$$= \omega_0 L/R$$

where $\omega_0^2 = 1/LC$.

(2) Q is also defined from the logarithmic decrease of amplitude in the damped harmonic motion. If δ is the logarithmic decrement

$$\delta = \pi/Q \qquad (3)$$

(3) Q is also defined as

$$\frac{1}{Q} = \frac{\Delta\omega}{\omega} \tag{4}$$

where $\Delta\omega$ is the half-width value of resonance and ω is the resonance frequency.

(4) The spatial attenuation function at a fixed time is given by $\exp(-\alpha x)$ where

$$\alpha = \omega/2cQ \tag{5}$$

Here $\omega = 2\pi f$, f being frequency and c is the phase velocity.

The attenuation as a function of time at a fixed point is given by $\exp(-\gamma t)$ where

$$\gamma = \omega/2Q \tag{6}$$

Knopoff (35) discussed the above definitions of Q and pointed out that in a homogeneous system without dispersion all the definitions are identical. However, in a strongly dispersed medium such as earth there are difficulties in relating the several definitions.

Both linear and non-linear models have been developed to take into account the deviations of the materials from perfect elasticity (35). Maxwell developed a linear model in which viscosity was introduced to describe creep under large deformations. In this model elastic strain and the rate of permanent strain are both proportional to stress. The specific dissipation function then comes

out to be

$$1/Q = \mu/\eta\,\omega \tag{7}$$

where μ = an elastic constant and η = a constant having the dimension of viscosity. Myer, Kelvin, and Voigt developed a linear model called the viscoelastic model. In this model the stress is the sum of two terms depending on the strain and the rate of strain. The specific dissipation function is then given by

$$1/Q = \omega\,\eta/\mu \tag{8}$$

Thus, the Myer-Kelvin-Voigt model gives the attenuation factor as a function of frequency squared, whereas in Maxwell's model the attenuation is independent of frequency.

In Boltzmann's linear superposition model the effect of each deformation is supposedly independent of previous or subsequent deformations. The total deformation of the solid is the sum of the partial deformations. The superposition model has not been extensively investigated because of the mathematical difficulties involved in the integral formulation.

Knopoff and MacDonald (36) developed a non-linear theory to explain the apparent constancy of $1/Q$ over a wide range of frequencies (about 10^{7} to 10^{-7} cps). However, as pointed out by Lomnitz (40) and MacDonald (44), this apparent constancy over a

wide frequency range can be explained by assuming an appropriate creep function in a linear theory.

The linear theory of dissipation has been worked out by various investigators (23, 36, 39, 60). Introducing complex elastic moduli, the specific dissipation function is defined as

$$1/Q = \frac{\text{imaginary part of the complex elastic modulus}}{\text{real part of the complex elastic modulus}} \qquad (9)$$

Using this definition, Yamakawa and Sato (60) deduced that the variable parts of an elastic modulus and viscosity coefficients are functions of each other. The same results were also obtained by Futterman (23) and Lamb (39) in analogy with Kramer-Kronig relations well known in electrical circuit theory.

To account for the diminution of amplitudes of a plane wave along the transmission path Futterman (23) gave the following equation for displacement amplitude for all time and space:

$$U(r,t) = U_0 \exp\left\{-\frac{\omega r}{2cQ}\left(1 - e^{-x}\right) + i\phi\right\} \exp(-i\omega t) \qquad (10)$$

where $U(r,t)$ = amplitude at distance r

U_0 = initial amplitude

ω = angular frequency

c = non-dispersive phase velocity

$1/Q$ = specific dissipation function

$$x = \omega/\omega_0$$

$$\phi = \omega r/V_p$$

$$V_p = c\left[1 - \frac{1}{\pi Q}\{\ln x + \ln\gamma\}\right]^{-1}$$

ω_0 = cut-off frequency (very low)

r = epicentral distance

t = time

$i = \sqrt{-1}$

$\log\gamma = 0.5772157$ = Euler constant

Since ω_0 was given by Futterman (23, p. 5286) as $2\pi x 10^{-3} sec^{-1}$, $x >> 15$ for the frequency range used (0.50 to 1.0 cps), the amplitude attenuation may be approximated by the term

$$\exp(-\omega r/2cQ)$$

since

$$(1 - \frac{1}{\pi Q}[\ln x + \ln\gamma])^{-1} \approx 1$$

$V_p \approx c$, and the phase is approximated by $\exp(\frac{i\omega r}{c})$ so that equation (10) reduces to

$$U(r,t) = U_0 \exp(\frac{-\omega r}{2cQ}) \exp(\frac{i\omega r}{c} - i\omega t) \qquad (11)$$

In this research, the amplitudes were transformed from the time to the frequency domain. When the amplitudes recorded at a particular position in space are replaced by Fourier transformed

amplitude A_{0_f} at the source and A_f at a distance r, and when $F(\xi)$ is the geometrical spreading loss which depends on epicentral distance, cycle of emergence and radius of the the earth and ϵ is the fractional loss at the interfaces, then

$$A_f = \epsilon F(\xi) A_{0_f} e^{-\omega r/2cQ} \tag{12}$$

This equation assumes that any difference in time due to the phase change of the amplitude is small compared to the total travel time r/c. Equation (12) can be expressed as

$$\log_e \frac{A_{0_f}}{A_f} = \frac{\pi f r}{cQ} - \log_e [\epsilon F(\xi)] \tag{13}$$

and

$$\frac{\partial}{\partial f} \log_e \frac{A_{0_f}}{A_f} = \frac{\pi r}{cQ} = \frac{\pi t}{Q}$$

where $t = r/c$ travel time from source to position in space.

Solving for Q yields

$$Q = \frac{\pi t}{\frac{\partial}{\partial f} \log_e \frac{A_{0_f}}{A_f}} \approx \frac{\pi t \Delta f}{\Delta \log_e \frac{A_{0_f}}{A_f}} \tag{14}$$

for small changes in frequency.

Thus the value of Q depends only on the slope of the $\log_e A_{0_f}/A_f$ versus frequency curve and travel time. For a narrow pass band of frequencies, Δf, the geometrical spreading and

interface losses can be considered to be constant.

Equation (14) indicates that Q is inversely proportional to the slope of the $\log_e A_{0_f}/A_f$ versus frequency curve.

Let

$$\frac{\Delta \log_e \frac{A_{0_f}}{A_f}}{\Delta f} = \beta \qquad (15)$$

$$\text{Therefore } Q = \pi t/\beta$$

$$\text{and } \partial Q = -\pi t \, \partial \beta/\beta^2$$

Since β is raised to the second power in the denominator and since larger values of Q are associated with smaller values of β for a given value of t, a given error in β will result in greater error for larger Q than in a smaller value of Q. Thus, it can be expected that uncertainty in values of Q will increase with increasing magnitude of Q.

Measurement of Absorptive Attenuation

Laboratory Observations. Collins and Lee (18), Howell (31), and Knopoff (35) have summarized the work done on the absorptive attenuation of seismic waves by earth materials. Most investigations were made by using high frequencies. The general result is that Q is substantially independent of frequency. This has been found to be the case for metals and non-metals too, except for

ferromagnetic materials.

However, there are also experimental results which show the dependence of Q on frequency. For example, Wegel and Walther's (58) investigations of the dissipation of energy in cylindrical rods of different materials excited by means of longitudinal and torsional vibrations show that Q is very close to a simple power function of frequency with exponents lying between $+1/2$ and $-1/3$ for different materials. Their results are applicable to a frequency range of 0.1 to 10^5 cps. Using a resonance method for study of attenuation and dispersion of the first longitudinal mode of propagation, and dispersion of the first flexural mode of propagation of elastic waves in a cylindrical rod of aluminum alloy, Zemanek and Rudnick (61) found that Q decreases monotonically from 2.5×10^5 to 1.2×10^5 as the frequency is increased from 0.84 to 100 kc. Born (12) found the logarithmic decrement to be independent of frequency for dry samples of sandstones, but a linear dependence as varying amount of water was injected into the sample.

Field Observations. Body waves, surface waves, and the free vibration of the earth have been used by various investigators to find the value of Q applicable to the inhomogeneous earth. The following is a list of some of the results obtained by them.

Table I. Q Values Obtained by Other Investigators

Investigator	wave type	period range (sec)	Q	reference
Gutenberg	Rayleigh	20	200	(24)
Ewing and Press	Rayleigh	140	150	(22)
Ewing and Press	Rayleigh	215	150	(22)
Gutenberg	P, PKP	4	1300	(27)
Gutenberg	P, PP	2	2500	(27)
Gutenberg	P, PP	12	400	(27)
Gutenberg	S	12	700	(27)
Gutenberg	S	24	400	(27)
Press	S	11	$\leq$500	(49)
Anderson and Kovach	S	25	508 and 400	(4)
Sato	LG	360-450	85-220	(54)
Båth and Lopez-Arroyo	L	75-300	90	(6)
BenMenahem	L	50-150	105	(7)
BenMenahem	R	50-150	145	(7)
Asada and Takano	P	1.0-0.143	400-4800	(5)

Anderson and Archambeau (2) have developed a method for the analysis of the amplitude of the dispersed wave trains and free oscillation of the earth which yeilds Q as a function of depth in the earth. Amplitude decay versus period for Love waves and torsional oscillations was computed by them for a variety of Q distributions in the earth. Those models which satisfied the available attenuation measurements have a broad highly attenuating

zone in the upper mantle (low Q) and a comparatively low attenuation in the lower mantle (high Q). The range of Q for shear waves in these models is from about 80 in the upper mantle to about 2000 in the lower mantle with rapid increase in Q beginning at about 400 km in depth.

Anderson, BenMenahem, and Archambeau (3) made an argument that Q for longitudinal waves should be about 2.4 to 2.6 times greater than that for shear waves. The values of Q for shear waves beneath the crust and at 400 km depth were found to be 60 and 150 respectively. Thus values of 150 and 375 would be expected for compressional waves if their argument is valid. Based on shear wave Q values computed by Kovach and Anderson (37) using frequencies between 0.015 and 0.07 cps, Q for compressional waves would be 1500 in the entire mantle, and 500 and 5500 for upper and lower mantle respectively. Knopoff (35) gave a value of 110 for Q of shear waves in the mantle applicable to 650 km in depth. According to the argument given by Anderson, BenMenahem, and Archambeau, Q values for P waves would be 275.

Computation of Q values have been made by various investigators using free vibration of the earth as a whole. Knopoff (35, p. 646) has listed those values with mode, period, reference and comments. Variations in Q values obtained by different

investigators for the same mode and period were found to be large.

AVAILABLE DATA

Data from four nuclear explosions were used for this research. Table II shows the pertinent data for these explosions. Recordings from other explosions were considered, but were rejected because the P wave amplitudes were too small at many of the distant stations. All of the explosions (Gnome, Haymaker, Bilby, and Shoal) were well-documented within 20 km range of the source and at teleseismic distances.

Close-in measurements (0-20 km) consisted of records obtained by strong motion instruments located on the surface of the ground and also by sub-surface instruments for the Gnome (16), Shoal, and Haymaker explosions (57). No sub-surface instruments recorded the waves from the Bilby explosion. Ground displacements calculated from records of sub-surface instruments were provided by Dr. Wendell Weart, Sandia Corporation. Records of ground particle displacements measured by surface instruments were provided by the U. S. Coast and Geodetic Survey. Plane views of the location of the strong motion instruments for Gnome, Shoal, and Haymaker are shown by Berg, Trembly, and Laun (9), and Trembly and Berg (57). Instrument locations for Bilby are shown in Figure I. For surface strong motion instruments, simple pendulum theory as given by Richter (50) is applicable for

Table II. Source Data for Explosions

Explosion and Date	Time of Detonation GCT	Location	Yield Kiloton	Depth of Burial feet	Type of Medium	Unified Magnitude	Reference
GNOME 10 Dec., 1961	19:00:00.0	32°15'49"N 103°51'57"W Carlsbad, New Mexico	3.1±0.5	1184	Salt	4.9±0.76	(53)
HAYMAKER 27 June, 1962	18:00:00.12	37°02'30"N 116°02'07"W NTS	56±8.0	1340	Alluvium	4.9	(41)
BILBY 13 Sept., 1963	17:00:00.13	37°03'38"N 116°01'18"W NTS	220±50.0	2314	Tuff	5.8	(42)
SHOAL 26 Oct., 1963	17:00:00.1	39°12'01"W 118°22'49"W Sand Spring Range, Nev.	12±2.0	1205	Granite	4.9	(43)

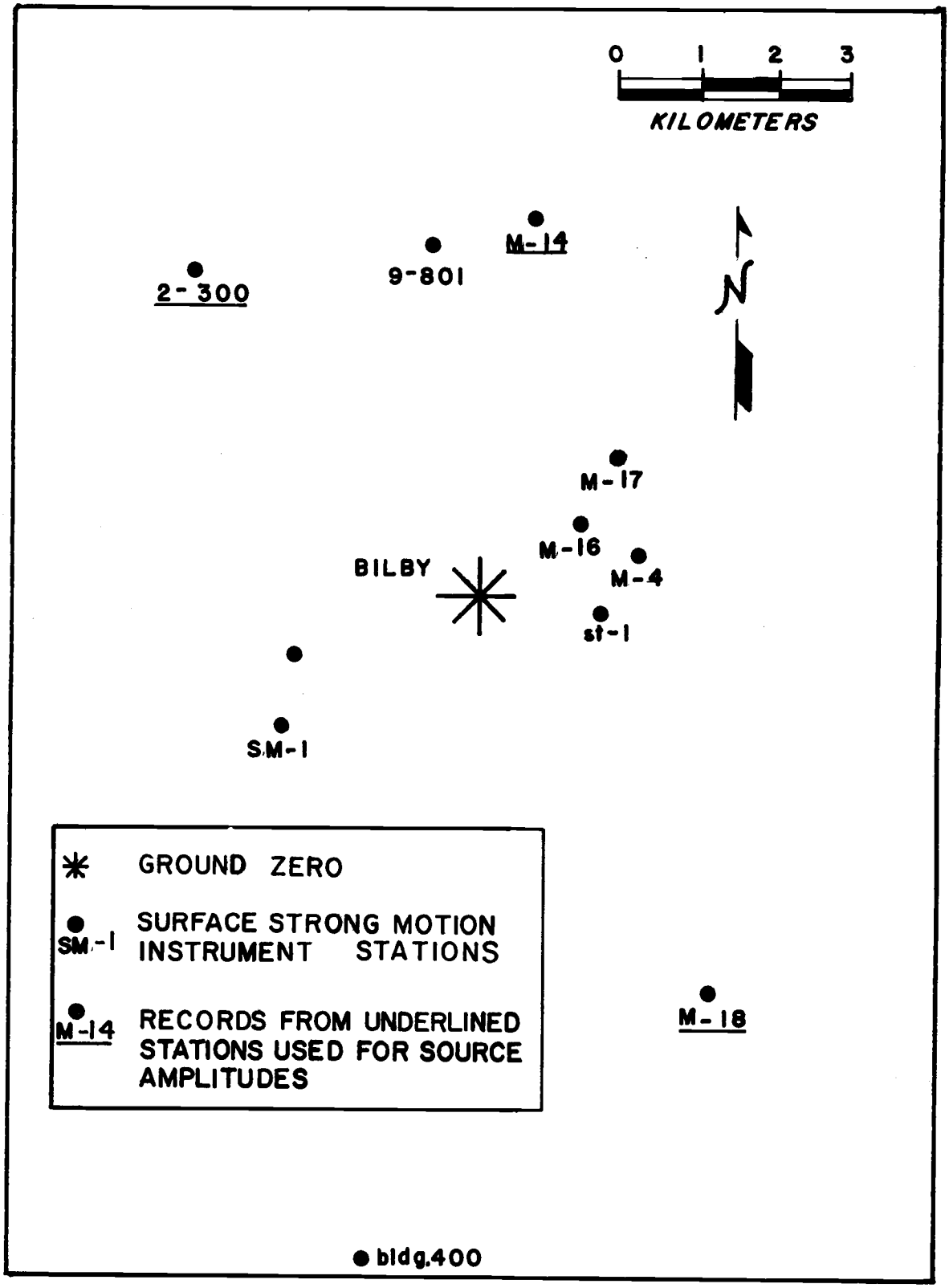

Figure 1. Plane view of the surface instrument locations for Bilby underground nuclear explosion.

calculating magnification and phase (Personal communications, U. S. Coast and Gedetic Survey), and these response characteristics are nearly flat in the frequency range of 0.5 to 1.0 cps.

Since only one component of measured ground motion is necessary to compute the confined ground motion at the surface station, the radial components of displacements were used for studies involving Gnome, Shoal, and Haymaker. However, the vertical components were also considered, in addition to the radial, for Bilby. The natural frequencies of the surface instruments were close to 0.25 cps for the radial, in all the cases, whereas the vertical components used for Bilby had natural frequencies close to 0.6 cps.

Different types of instruments recorded the first P arrival at epicentral distances between 9° and 91° which was the range of teleseismic recordings considered for this study. Seismograms recorded by vertical seismographs were used in all the cases, except for Blacksburg (Bilby) and Atlanta (Shoal) where East-West components were used because the vertical components were too noisy. Most of these were short period (S. P.) Benioff type instruments, but some were Willmore (S. P.), Grenet (S. P.), Hiller, and SVSN-4 type instruments. Records were used only from those stations whose instrument response curves were known.

Selection of the records was based on the clarity of the first

arrival. A few examples of the quality of records that were used and those which were rejected are shown in Figure 2. Distribution of the explosion sites and the distant recording stations that were used are shown in Figure 3. Table III gives the pertinent information about the seismograph stations and the recordings of the nuclear explosions. The station locations, Co-ordinates, events recorded, and type of instruments used are shown in Appendix I.

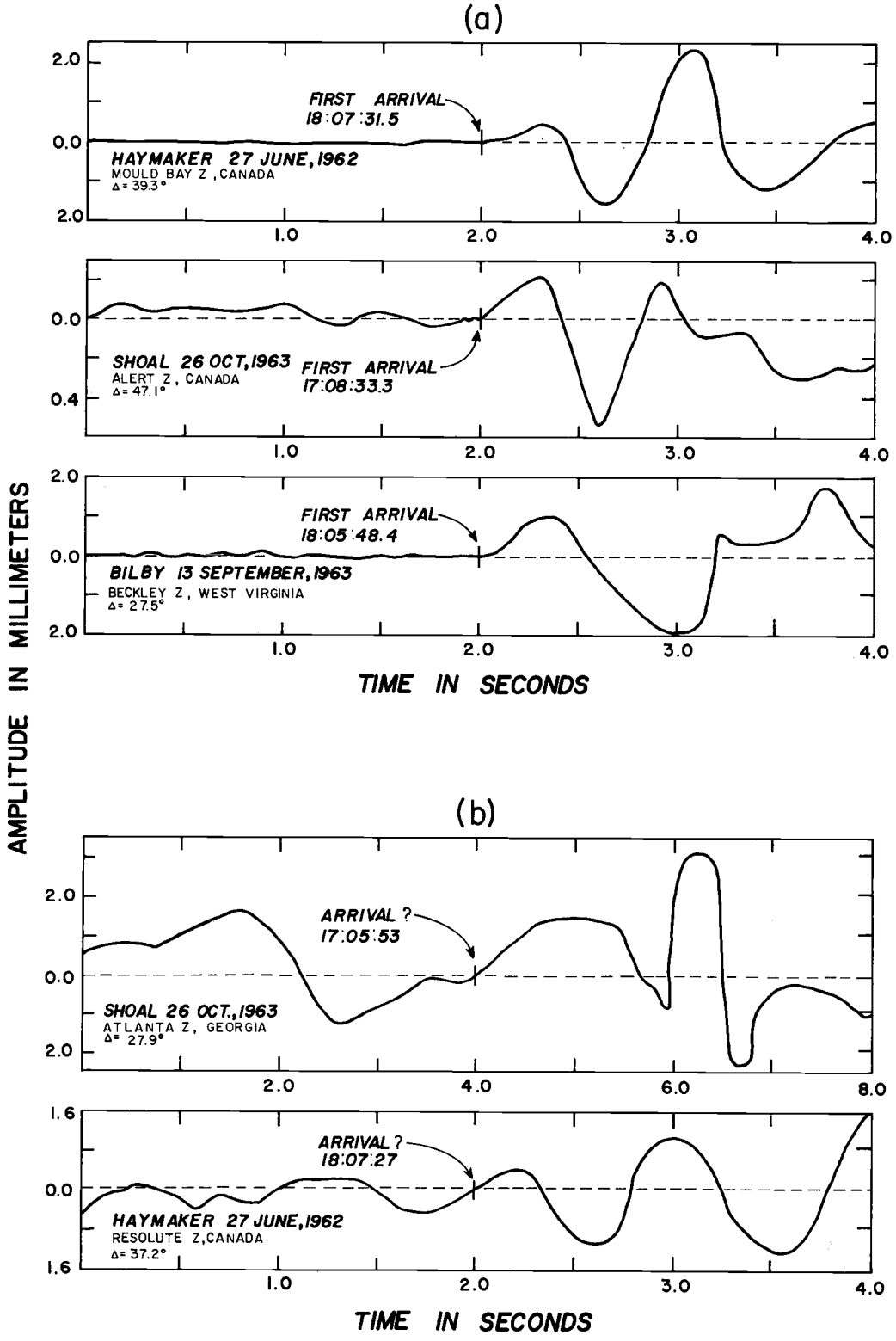

Figure 2. Examples of quality control.
(a) Records used in this research
(b) Records not used in this research

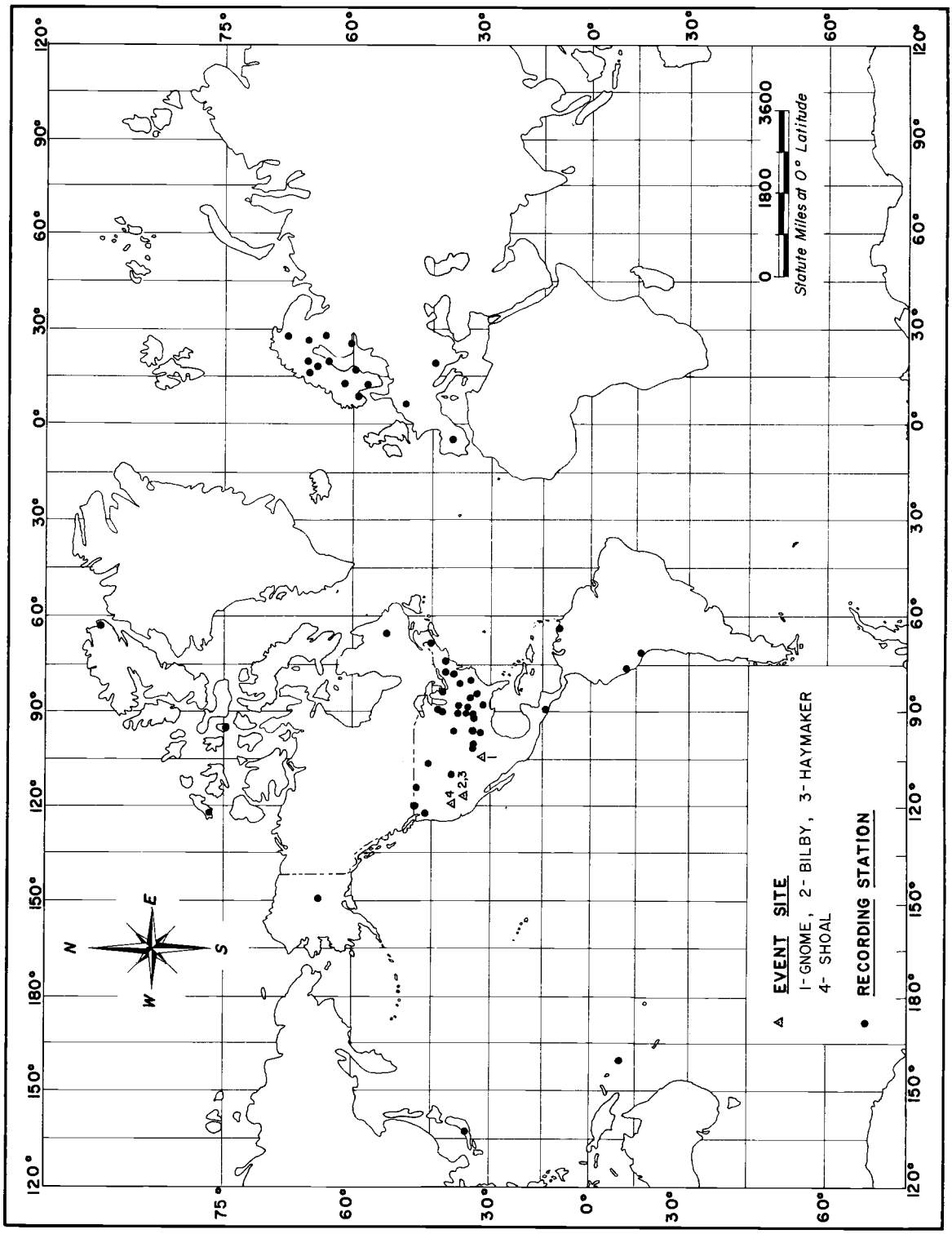

Figure 3. Diagram showing the locations of the explosions and recording stations.

Table III. Informations About Records from Nuclear Explosions Used for this Research

Explosion	Station	Δ* in km	Δ* in degree	observed travel time in sec.	Azimuth from source in Degrees	Deviations from Jeffreys-Bullen travel times (J. B. -observed) in sec.
Bilby	Longmire	1178. 19	10. 59	156. 70	337. 70	-0. 6
	Hungry Horse	1265. 10	11. 38	166. 60	6. 80	0. 3
	Forsyth	1281. 60	11. 53	166. 00	35. 70	2. 9
	Tonasket	1335. 82	12. 01	175. 20	384. 50	0. 1
	Shamrock	1425. 80	12. 82	187. 80	94. 60	-1. 5
	Manhattan	1717. 90	15. 40	219. 30	76. 50	0. 9
	Durant	1831. 00	16. 40	229. 90	95. 00	3. 1
	Rolla	2132. 80	19. 20	266. 00	80. 40	1. 8
	Florissant	2256. 44	20. 30	278. 70	77. 20	1. 4
	St. Louis	2269. 15	20. 40	280. 00	77. 90	1. 2
	Dubuque	2299. 25	20. 68	277. 30	66. 80	1. 8
	Eutaw	2606. 16	23. 40	311. 70	92. 30	-0. 4
	Cumberland Pl	2727. 66	24. 50	322. 00	84. 40	0. 0
	Ann Arbor	2819. 93	25. 30	328. 70	68. 20	0. 9
	Atlanta	2892. 20	26. 10	336. 00	88. 70	1. 1
	Beckley	3056. 00	27. 48	348. 40	77. 80	1. 4
	Blacksburg	3146. 00	28. 30	356. 10	79. 00	1. 4
	Berlin	3236. 00	29. 11	363. 00	72. 82	1. 5
	State College	3308. 78	29. 70	368. 30	71. 00	1. 5
	LaPalma	3665. 05	33. 00	397. 70	126. 50	1. 1
	Houlton	4066. 00	36. 56	427. 70	60. 30	1. 6
	Schefferville	4189. 60	37. 60	436. 30	45. 90	1. 7
	Resolute	4340. 10	38. 90	447. 30	8. 80	1. 7
	Mould Bay	4372. 00	39. 20	451. 40	358. 70	0. 1
	Alert	5437. 97	48. 80	526. 30	8. 10	2. 5

Table III. (Continued)

Explosion	Station	Δ in km	Δ in degree	observed travel time in sec.	Azimuth from source in Degrees	Deviations from Jeffreys-Bullen travel times (J. B. -observed) in sec.
Bilby	Caracas	5791. 92	51. 40	547. 70	108. 10	0. 9
	Nana	6796. 51	61. 20	616. 60	135. 10	2. 3
	Kevo	7797. 07	70. 30	672. 50	12. 90	4. 7
	Kiruna	7829. 46	70. 41	675. 20	16. 10	2. 7
	Skalstugan	7967. 04	71. 65	682. 80	21. 70	2. 6
	Sodankyla	8015. 26	72. 11	685. 10	14. 30	2. 4
	Umea	8190. 71	73. 66	694. 30	18. 70	2. 9
	Konsberg	8198. 70	73. 73	695. 40	25. 50	1. 5
	Kajaani	8361. 03	75. 19	703. 60	15. 60	2. 5
	Goteborg	8452. 02	76. 01	708. 60	25. 90	2. 7
	Uppsala	8467. 74	76. 15	709. 10	22. 10	2. 4
	Nurmi jarvi	8625. 57	77. 60	717. 30	18. 70	2. 3
	Karlskrona	8723. 51	78. 45	722. 00	25. 30	2. 3
	Bensberg	5803. 64	79. 20	727. 20	32. 60	0. 6
	Matsushiro	8850. 53	79. 60	729. 20	308. 00	1. 3
	Toledo	9029. 70	81. 21	738. 30	46. 20	0. 8
	Pruhonice	9225. 16	82. 96	747. 10	29. 60	1. 1
	Honiara	10107. 07	90. 90	785. 80	258. 90	1. 0
Gnome	Vernal	1048. 27	9. 43	141. 70	332. 39	-4. 6
	Conway	1146. 28	10. 31	147. 00	70. 63	5. 2
	Jackson	1457. 30	13. 10	184. 30	70. 88	5. 7
	Resolute	4751. 56	42. 73	477. 50	3. 50	3. 0
	Mould Bay	4965. 80	44. 66	494. 00	354. 8	2. 1
Haymaker	Rolla	2135. 00	19. 20	266. 20	80. 40	1. 6
	Madison	2335. 00	20. 86	286. 30	67. 08	-0. 3
	Mould Bay	4371. 86	59. 31	451. 50	358. 75	0. 9
	Alert	5440. 24	48. 93	526. 60	8. 09	3. 1

Table III. (Continued)

Explosion	Station	Δ in km	Δ in degree	observed travel time in sec.	Azimuth from source in Degrees	Deviations from Jeffreys-Bullen travel times (J. B. -observed) in sec.
Shoal	Hungry Horse	1075.00	9.67	143.00	17.20	-7.4
	Manhattan	1874.45	14.80	239.10	83.00	-1.1
	Dallas	2064.17	18.30	260.10	103.30	-0.7
	Rolla	2307.99	20.70	283.30	85.10	1.0
	Florissant	2417.73	21.70	293.90	82.10	0.6
	Oxford	2623.00	23.50	313.10	92.40	-0.8
	Atlanta	3104.00	27.92	352.40	91.20	1.4
	College Cut Post	3436.18	30.90	379.70	335.90	1.6
	Ogdensberg	3749.10	33.20	398.60	72.50	1.9
	Resolute	4139.61	37.20	434.90	10.00	-0.2
	Mould Bay	4131.00	37.20	434.30	359.60	0.4
	Alert	5232.92	47.10	513.40	8.60	2.1
	Arequipa	7849.48	70.50	678,90	132.10	-0.5

* Δ = epicentral distance.

ANALYSIS OF DATA

Prior to the time of underground nuclear explosions, records from earthquakes were the only data available for the study of compressional wave attenuation in the earth's mantle. Since the source functions of the earthquakes were not known, assumptions had to be made regarding source amplitude spectra, or the source amplitude function had to be eliminated in order to compute the absorption of seismic compressional waves in the earth's mantle. The advantage of underground nuclear explosions over earthquakes for this kind of study is that compressional P waves from such explosions are recorded from very close to the point of explosion to the teleseismic distances, and in many cases the source function can be computed.

Previous Methods of Analysis

Gutenberg (24, 27) computed the value of Q by the observed broadening of a pulse from station to station. If x and y are two waves such as P and P'P' or P'P'P' travelling distances D_x and D_y respectively, H is the amplitude ratio computed from theoretical equations, T is the period, and r is the observed amplitude ratio, then

$$K = \frac{2\pi}{QTV} = 2(\log H - \log r)/(D_x - D_y)\log e \qquad (16)$$

The absorption term used in the above equation is given by

$$a = e^{-KD} \qquad (17)$$

Kovach and Anderson (37) used the amplitudes of the multiple core reflections of shear waves emitted by deep focus earthquakes to compute Q. Amplitudes of these multiple reflections were combined to estimate the reflection coefficient at the core-mantle boundary. Assuming the energy radiated in the upward and downward direction to be same, they could estimate the value of Q for shear waves in the mantle.

Asada and Takano (5) studied the spectra of P waves emitted by earthquakes of different focal depths to compute Q. Assuming a relation of the type

$$A = A_o \exp\left(-\frac{\pi f r}{QV}\right) \qquad (18)$$

and assuming that the amplitude spectrum at the source was inversely proportional to the frequency, different Q values were used in equation (18) to match the smoothed observed and theoretical spectra. The value for which the matching was best was taken as the representative Q value.

Method of Analysis Used in This Research

In this research the following equation was used to compute values of Q applicable to the mantle of the earth for compressional waves with frequencies between 0.5 and 1.0 cps:

$$Q = \frac{\pi t \ \Delta f}{\Delta \log_e A_{0_f}/A_f} \tag{14}$$

In this equation the logarithm of the ratio of the Fourier transformed amplitude of the displacement pulses measured near the source to that of the corresponding P arrival recorded beyond 9° epicentral distance was plotted against frequency. The plot of $\log(A_{0_f}/A_f)$ versus frequency will be a straight line if Q is constant in the range of frequencies under consideration. Sample plots of data from this research are shown in Figure 4. The plots of data have only a little curvature between 0.5 and 1.0 cps. Best possible straight lines were drawn through points from 0.5 to 1.0 cps and from 0.7 to 1.0 cps by the method of the least mean squares, and the slopes of the straight lines were used to compute Q by using equation (14). Hence, Q is considered to be constant in the ranges of the frequencies considered.

The assumed frequency independent terms (geometrical spreading factor and the interface losses) involved in equation (12) drop out of the computations of Q. Further, the instrument

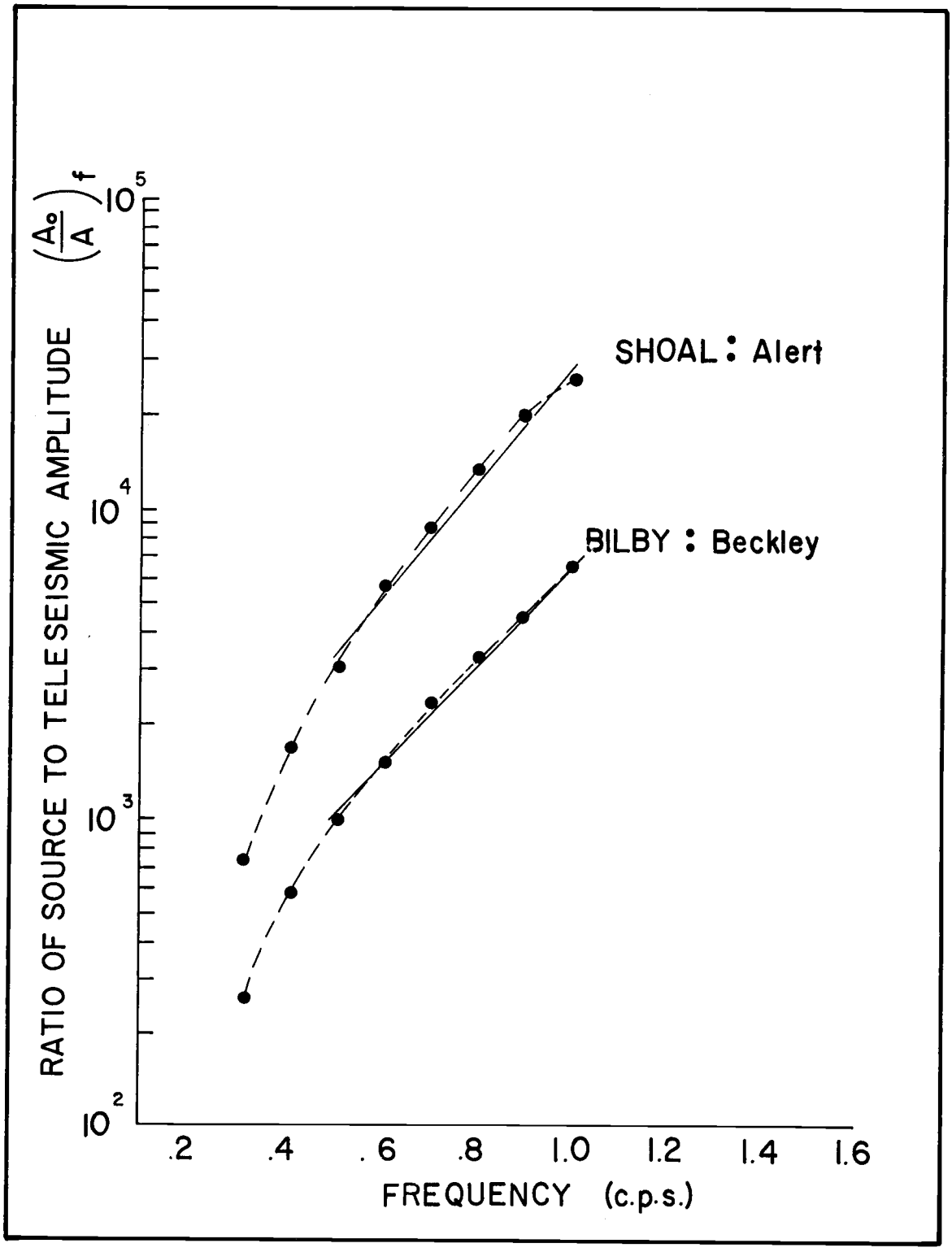

Figure 4. Sample plots of log A_o/A versus frequency.

magnification at 1 cps is not critical since Q depends on the variation of the amplitude ratio with frequency and not on absolute amplitude. Therefore, the accuracy of the computed values of Q will depend on the accuracy of the frequency response curves as well as the quality of the recordings. The Q values obtained by this method are lumped Q values; that is, a given value of Q is the average for the entire propagation path of the wave.

Because of uncertainty in the low frequency cut-off of the response curves for the instruments used in Rolla, St. Louis, Dubuque, Manhattan, and College Outpost, Q was computed in the frequency range of 0.7 to 1.0 cps for P arrivals recorded at these stations. In all other cases two frequency bands 0.5 to 1.0 cps and 0.7 to 1.0 cps were considered. The changes in frequency response characteristics from the time of calibration to the times of recordings are not known.

Discussion of the Method of Analysis

To use equation (14) effectively for computing Q, many special considerations had to be given to the data from the nuclear explosions. The following topics were investigated in detail and a brief discussion of each is given below: (1) Distance of source measurement; (2) Source signal; (3) Teleseismic signal; (4) Interference from other signals; and (5) Travel time of teleseismic

signals.

Distance of Source Measurement. Berg, Trembly, and Laun, and Trembly and Berg have studied the primary waves very close to the sources for Gnome, Shoal, and Haymaker nuclear explosions. Berg and Papageorge (8) gave a detailed analysis of the theoretical seismic source given by Blake (1952) for explosions. The above works showed the presence of a long period field which dies off as the inverse square of the distance from the source. The presence of the long period field in recordings from nuclear explosions has been confirmed by Berg, Trembly, and Laun, and Trembly and Berg. Figure 5 shows this effect for the Bilby nuclear explosion. At a short distance from the source, the energy contribution of the long period field is less than that of the radiation field which diminishes as the inverse distance. Thus, amplitudes in the spectrum of the radiation field are of direct concern in this research. The Fourier transformed amplitudes of the displacement pulses recorded at 9.47, 9.66, and 12.60 km from the shot point for Gnome, Shoal, and Haymaker respectively and at 9.82, 11.63, and 11.87 km for Bilby were used as source amplitudes in this research. At these distances the contribution of the long period field is small and hence only the radiation field is important.

Source Signal. It has been shown in the references cited above that the first half-cycle of the records from the surface

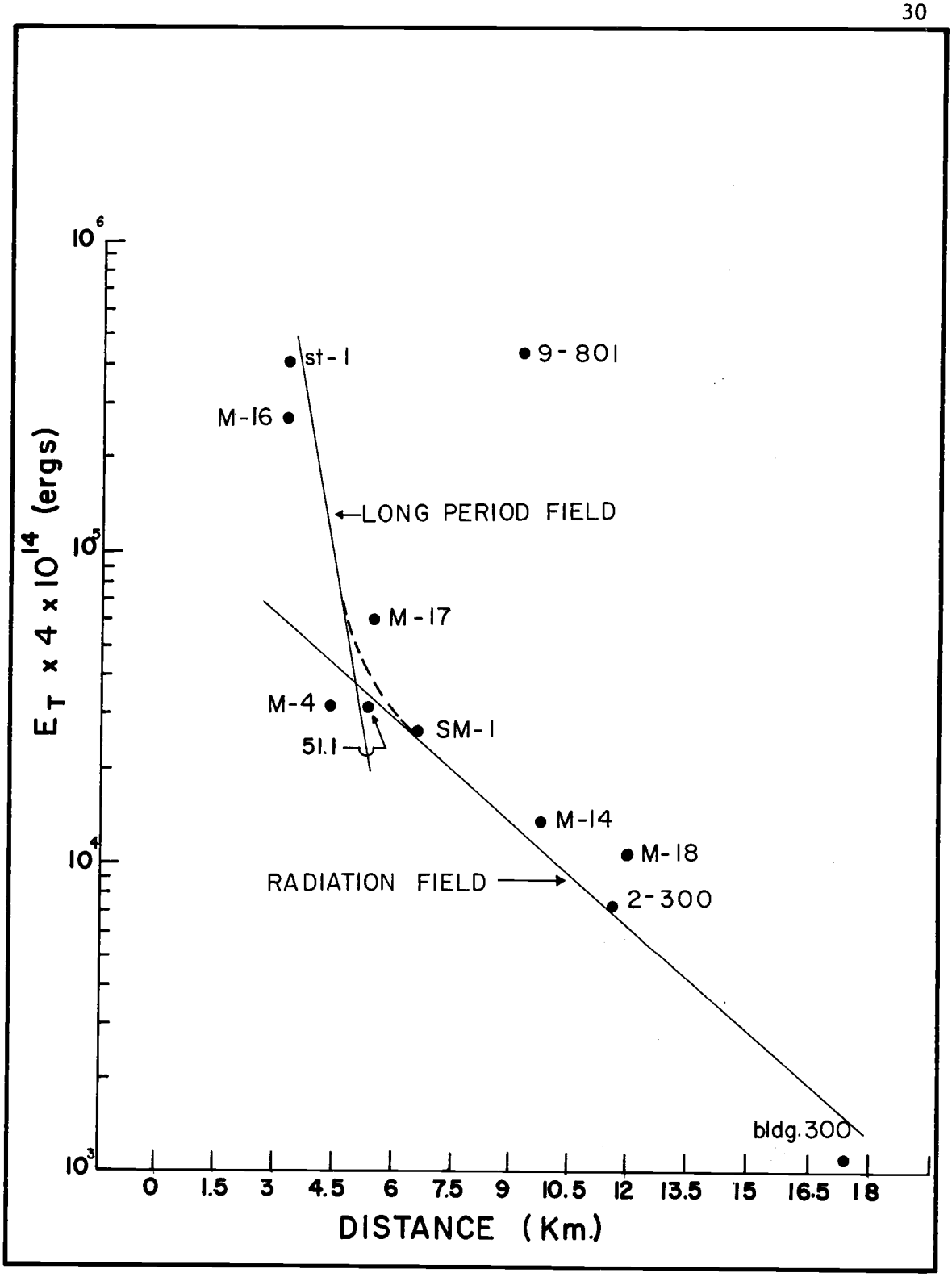

Figure 5. Variation of energy (E_T) of first half-cycle of ground motion with distance for the Bilby underground nuclear explosion.

instruments contained an estimated 75 percent of the energy of P wave and that beyond the first half-cycle the pulses were influenced by other arrivals. The theoretical pulses for Gnome and Shoal were propagated to a distance of 10.0 km, and that for Haymaker was propagated at 12.6 km. At these distances or very close to them observations were made of the first P arrival for comparison with the theoretical pulses. Figure 6 shows that the theoretical pulses consist of one cycle with major part of energy in the first half-cycle. The Fourier transformed amplitudes $g(\omega)$ of these pulses compared very well with those of the first half-cycles of the recorded waves for Gnome and Shoal, and first cycle for Haymaker in the frequency range of 0.5 to 1.0 cps. The theoretical spectra had to be multiplied by constants in each case to make the transformed amplitude comparable to that of the recorded pulses because of theoretical considerations. The results of this analysis are shown in Figure 7.

For Bilby explosion no sub-surface station record was available at close range and hence no theoretical source was used. However, the energy content of the first half-cycles of the first P arrival recorded by the surface instruments computed in the same manner as Berg, Trembly, and Laun shows the presence of a long period field in addition to the radiation field when plotted against distance. This long period field diminishes rapidly with distance so that beyond about 10.0 km its contribution to the total energy is

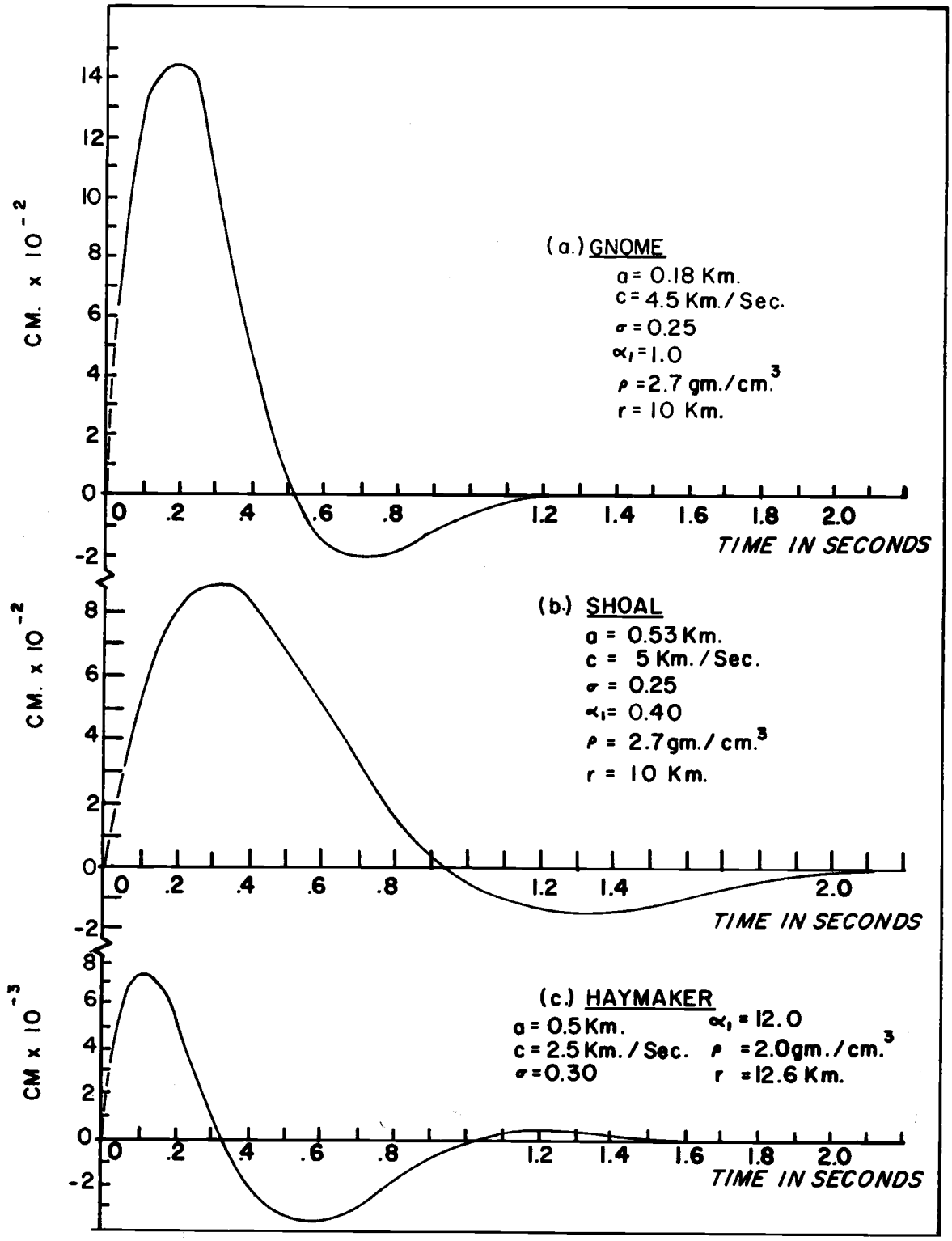

Figure 6. Displacement pulses showing theoretical source amplitude as a function of time.

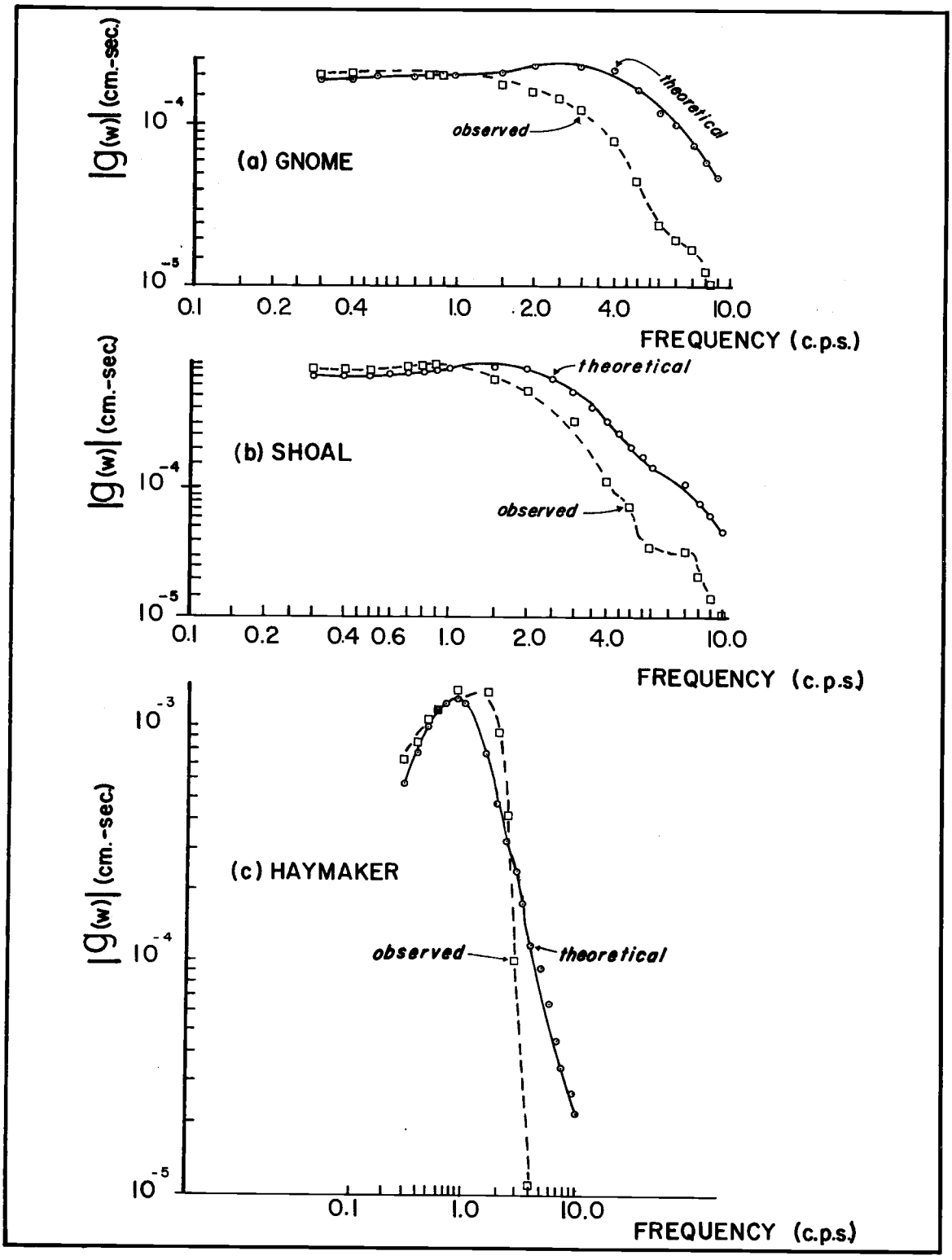

Figure 7. Comparison of Fourier transformed amplitudes $g(\omega)$ for observed and theoretical displacement pulses.

less than one percent (Figure 5). Very close to this distance and beyond records of measured ground motion were available to use as source records for Bilby. Table IV summarizes the source information used in this research. The displacement pulses used here are shown in Appendix II.

Table IV. Source Amplitude Data

Explosion	distance of the recording station km	component used	number of cycles used
Gnome	9.47	radial	first half cycle
Shoal	9.66	radial	first half cycle
Haymaker	12.60	radial	first cycle
Bilby	9.82	radial	first half cycle
Bilby	9.82	vertical	first cycle, and first one and half cycles
Bilby	11.63	radial	first cycle
Bilby	11.87	vertical	first cycle

Teleseismic Signal. The first P arrival recorded by vertical seismographs at a distance beyond 9° epicentral distance consists, in general, of several cycles of oscillations lasting sometimes for several seconds. It is suspected that these oscillations may be the resultant of several pulses for the following reasons:

(a) Records from instruments located close to the source show several arrivals within one second of the zero time (see

Appendix III). If these later arrivals were due to source mechanism and if there was a free surface reflection, an additional pulse might have been propagated along the same path as the direct wave and by interference produced the observed oscillations.

(b) The first P arrival recorded by some stations at teleseismic distances could be separated into three pulses: that is, direct, reflected, and a compressional pulse with a time delay (see Appendix III).

(c) Werth, Herbst, and Springer (59) computed the theoretical wave forms for the first cycle and a half for distances of 96 to 714 km from several nuclear explosions. Using propagation parameters based on crustal models and convolving the effects of attenuation and instrument response with the source function, they calculated the theoretical displacement amplitude, the first cycles of which agreed with the experimental measurements of the Logan and Blanca explosions within +4 to -16 percent. They postulated that the wave form of the first P wave was influenced by non-linear type of surface reflections.

(d) Particle motion diagram for some records show that the first P arrival is affected by some new arrival in the second and third half-cycles. Figure 8 shows some illustrations of this fact.

(e) In the records of Bilby a distinct second arrival of compressional type occurred within one and two seconds from the

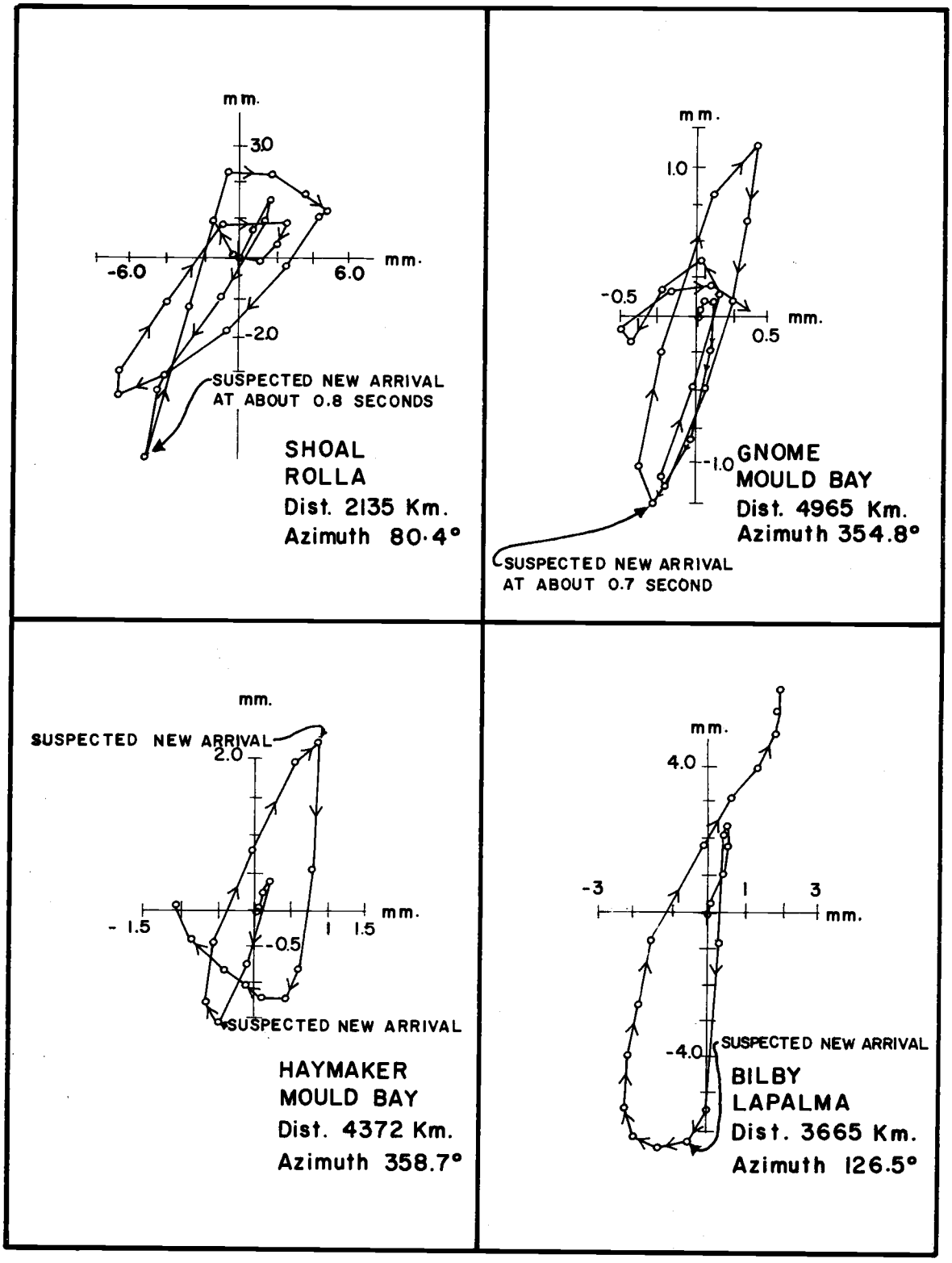

Figure 8. Particle motion diagrams for first arrival P pulses recorded at teleseismic distances.

onset. It influenced the third half-cycle in many cases. To determine the effect of considering different length of the initial P arrival on the computed Q values, the theoretical displacement function for Gnome was computed at a distance of 3000.0 km. The cavity radius was adjusted in such a manner that the natural frequency of the cavity was close to 1 cps for a propagational velocity of 8.5 km/sec. The resulting theoretical pulse was then filtered through a short period Benioff, using the instrument response curve supplied by the U. S. Coast and Geodetic Survey. The filtered pulse looks very similar to that recorded at teleseismic distances from a nuclear explosion. The filtered and unfiltered pulses are shown in Figure 9. The Fourier transformed amplitudes of the first one cycle, first one and half-cycles, and two cycles for the filtered pulse are shown in Figure 9(c). They agree closely for the frequencies above 0.5 cps for this particular case. Theoretically, this analysis shows that the length of the pulse is not too critical for Q as computed in this research. Theoretical studies mentioned above tend to indicate that the true pulse of the first arrival P waves recorded by a Benioff consists of three half-cycles with the third half-cycle amplitude much smaller than the second half. Considering all these facts, the computations of Q were made by using the transformed amplitudes of the (a) first cycle (b) first one and half cycle of the recorded wave and (c) the

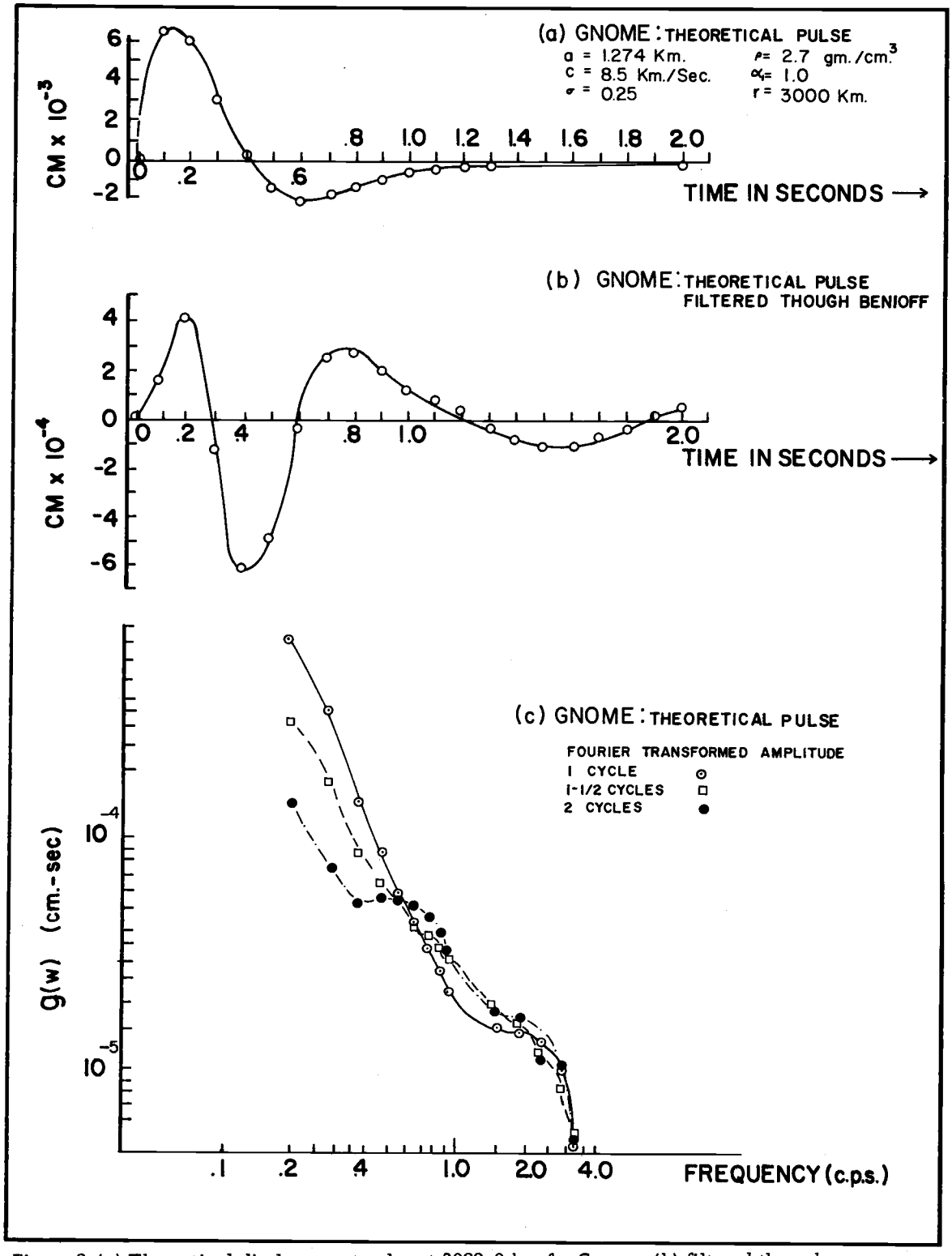

Figure 9. (a) Theoretical displacement pulse at 3000.0 km for Gnome; (b) filtered through a Benioff short period vertical seismometer (pass band 0.10 to 10.0 cps); (c) Fourier transformed amplitude $g(\omega)$ of 1 cycle, 1 1/2 cycles, and 2 cycles of the filtered pulse corrected for instrument magnifications.

first arrival refined by removing the surface reflection as mentioned above. Henceforth the wave refined by removing the surface reflection will be called the direct wave.

The separation of the pulses, assuming surface reflection, by the method described above, was possible only in two stations out of thirteen in Shoal, two out of four in case of Haymaker, one out of five in Gnome, and seven out of forty-three in Bilby. Most of these stations where separation was possible lie in the North-East quadrant between 2000 and 4000 km distance range.

Interference Due to Refraction Signals from Deep Horizons

Computations of Q were made by assuming that the layering of the earth did not alter the mode of propagation of the first P arrival between 9° and 91° epicentral distance. This would allow a comparison of the Q values applicable at different distances. The extent to which this assumption is true is not known.

A simple computation was made to determine the difference in epicentral distance necessary to eliminate interference between two refraction arrivals. Assuming layers of constant velocities, the time distance equation for a refraction arrival is

$$T = \frac{X}{V} + C \qquad (19)$$

where V is velocity below the interface in question, T is the travel time, X is the epicentral distance, and C is a constant

involving the velocities above and below the interface.

The step-out time for the arrival is

$$dT/dX = 1/V \tag{20}$$

If a refraction arrival is observed propagating with an apparent velocity of 8.0 km per second and at a given time a new refraction arrival is observed that propagates with an apparent velocity of 8.5 km per second, the two arrivals would separate by about 2 seconds in 100 km.

Thus, a P arrival at a given station may be affected by interference with another arrival, but the pulses should separate enough in 100 km to eliminate interference effects in computed values of Q. The value of Q at any particular station may be questioned on the basis of interference, but trends in Q which persist over a hundred kilometers should have a minimum of interference effect.

Travel Time

Travel time to a particular station enters the computation of Q because of the term r/c in equation (12). However, the computations are not sensitive to variations of a few seconds because of the magnitude of the travel time. For this reason, times read directly from the records were used in computing the values of Q.

Errors in Q resulting from variations in time are less than 2 percent. Table III gives the travel times and corresponding deviations from Jeffreys-Bullen travel times for P waves of surface focus earthquakes (34).

To summarize, the Fourier transformed amplitude of the first half-cycle in case of Gnome and Shoal, and one cycle in case of Haymaker of the recorded radial displacement pulses at 9.47, 9.66, and 12.6 km, respectively, were used as source amplitudes in the term A_{0_f}, for a particular frequency f. In case of Bilby, several displacement pulses of different lengths were considered for source amplitude (see Table IV). Fourier transformed amplitudes of the first cycle, first one and half cycles, and of the direct waves of the first P arrivals recorded beyond 9° epicentral distances were corrected for instrument magnification and free surface effects. The resulting amplitudes in the frequency domain were used as the values of A_f.

The slope of the logarithm of the ratio of source amplitude to the distant amplitude versus frequency curve (i.e., $\log A_{0_f}/A_f$ versus frequency) was obtained by the method of least mean squares in the frequency range of 0.5 to 1.0 cps and 0.7 to 1.0 cps. Using the slope thus obtained and travel time, Q was computed using equation (14).

PRESENTATION OF RESULTS

If the interior of the earth were homogeneous, the factor Q would be related to the epicentral distance in a relatively simple manner. However, any deviation from homogeneity of the material in the interior--in the horizontal or vertical direction--would make the variation of Q with epicentral distance complicated. So the variation of Q with epicentral distance should give an indication of the inhomogeneity of the interior of the earth.

Q Versus Epicentral Distance

The apparent Q values computed in this study are listed in Tables V and VI. The tables show the Q values computed by taking the first cycle, first 1 1/2 cycles and the direct wave in the frequency ranges of 0.5 to 1.0 cps and 0.7 to 1.0 cps. Each Q value for Bilby is an average of the values obtained by taking different displacement pulses as the source function. Figure 10 shows the plot of Q versus epicentral distance for one cycle in the frequency range of 0.7 to 1.0 cps. The numbers within parentheses represent Q values obtained for 1 1/2 cycles of the recorded pulse. Q values for the direct waves are underlined. There seems to be considerable scatter in the values for Qs. However, those computed using one cycle lie within the envelope represented

Table V. Average Q for 0.5-1.0 cps

Explosion	Station	Distance in km	Distance in degree	1 cycle	1 1/2 cycles	Direct Wave
Bilby	Longmire	1178. 19	10. 59	88. 97±13. 4	98. 6±16. 4	
	Hungry Horse	1265. 10	11. 38	106. 6±18. 2	127. 9±25. 8	
	Forsyth	1281. 60	11. 53	117. 8±22. 3		
	Tonasket	1335. 82	12. 01	101. 6±15. 7		
	Shamrock	1425. 80	12. 82	127. 4±22. 6	145. 8±29. 1	160. 3±34. 7
	*Manhattan	1717. 90	15. 40	*		
	Durant	1831. 00	16. 40	132. 9±20. 6		
	*Rolla	2132. 80	19. 20	*		
	Florissant	2256. 44	20. 30	223. 7±45. 8		
	*St. Louis	2269. 15	20. 40	*	*	
	*Dubuque	2299. 25	20. 68	*	*	
	Eutaw	2606. 16	23. 40	213. 8±39. 6		
	Cumberland Pl	2727. 66	24. 50	152. 9±19. 4		
	Ann Arbor	2819. 93	25. 30	283. 3±61. 9		
	Atlanta	2892. 20	26. 10	325. 5±78. 5	274. 5± 57. 6	
	Beckley	3056. 00	27. 48	251. 2±46. 5		353. 0±88. 2
	Blacksburg	3146. 00	28. 30	232. 3±40. 5		
	Berlin	3236. 00	29. 11	266. 3±119. 7	285. 1±57. 4	
	State College	3308. 78	29. 70	326. 0±72. 1	300. 7±61. 9	
	LaPalma	3665. 05	33. 00	278. 7±50. 9	159. 9±17. 6	
	Houlton	4066. 00	36. 56	291. 2±51. 2		316. 0±60. 4
	Schefferville	4189. 60	37. 60	339. 2±70. 8	393. 0±89. 2	452. 4±121. 5
	Resolute	4340. 10	38. 90	287. 1±75. 4	294. 5±50. 6	
	Mould Bay	4372. 00	39. 20	210. 9±26. 5	254. 5±38. 3	
	Alert	5437. 97	48. 80	375. 7±99. 3		
	Caracas	5791. 92	51. 40	401. 7±126. 5	482. 2±107. 2	
	Nana	6796. 51	61. 20	446. 4±83. 8		
	Kevo	7797. 07	70. 30	615. 1±138. 6	886. 2±369. 8	
	Kiruna	7829. 46	70. 41	876. 9±276. 3	5492. 2±?	
	Skalstugan	7967. 04	71. 65	778. 8±215. 2		
	Sodankyla	8018. 26	72. 11	514. 6±96. 2	758. 3±207. 4	

Table V. (Continued)

Explosion	Station	Distance in km	Distance in degrees	1 cycle	1 1/2 cycles	Direct Wave
Bilby	Umea	8190.71	73.66	589.8±123.2		865.6±261.8
	Konsberg	8198.70	73.73	631.3±147.6	834.0±242.3	
	Kajaani	8361.03	75.19	650.4±150.9	840.9±243.5	
	Goteborg	8452.02	76.01	1025.6±358.6		
	Uppsala	8467.74	76.15	789.0±215.0	1675.5±956.5	
	Nurmijarvi	8625.57	77.60	587.5±122.8	704.6±171.7	
	Karlskrona	8723.51	78.45	901.2±278.8	1374.7±527.8	
	Bensberg	8803.64	79.20	910.2±276.1	527.3±86.1	
	Matsushiro	8850.53	79.60	1615.0±867.2	4489.6±?	
	Toledo	9029.70	81.21	609.0±128.0	525.5±134.9	
	Pruhonice	9225.16	82.96	666.9±151.3		
	Honiara	10107.07	90.90	565.6±112.4	669.1±144.5	
Gnome	Vernal	1048.27	9.43	112.8		
	Conway	1146.28	10.31	149.2	170.2	
	Jackson	1457.30	13.10	151.9		
	Resolute	4751.56	42.73	283.0	172.0	
	Mould Bay	4965.80	44.66	230.0	281.5	269.0
Haymaker	*Rolla	2135.00	19.20	*	*	*
	Madison	2335.00	20.86	200.0	267.0	
	Mould Bay	4371.86	39.31	200.0	225.0	334.0
	Alert	5440.24	48.93	309.2	317.0	
Shoal	Hungry Horse	1075.00	9.67	144.7	256.3	
	*Manhattan	1874.45	16.80	*	*	*
	Dallas	2064.17	18.50	315.3	580.9	
	*Rolla	2307.99	20.70			
	Florissant	2417.73	21.70	341.0	694.7	
	Oxford	2623.00	23.50	317.1		
	Atlanta	3104.00	27.92	335.5	472.0	
	College Out Post	3436.18	30.90	*		

Table V. (Continued)

Explosion	Station	Distance in km	Distance in degrees	1 cycle	1 1/2 cycles	Direct Wave
Shoal	Ogdensberg	3749.10	33.20	427.9	728.6	
	Resolute	4139.61	37.20	286.6	205.0	
	Mould Bay	4131.00	37.20	222.7	280.6	340.0
	Alert	5232.92	47.10	381.7	435.2	
	Arequipa	7849.48	70.50	856.4	1471.2	

*computed for .7-1.0 cps. only.

by two dashed lines. The two dashed lines show almost identical peaks and troughs at almost the same epicentral distance. The lowest values of Q occur at the beginning of the envelope, and there is a general trend of increasing Q with epicentral distance up to about 80°, beyond which there seems to be a sharp decrease to at least 91° epicentral distance. In general, higher values of Q are obtained when computations are made by using 1 1/2 cycles and direct waves rather than one cycle of the initial P arrivals, except for the pulses recorded in Atlanta, State College, LaPalma, Bensberg and Toledo for Bilby; and Resolute for the Gnome and Shoal explosions. The increase in Q values because of using 1 1/2 cycles or direct waves in lieu of the first cycle occurs near the peaks only. As a result, the general trend of the envelope remains unaltered regardless of the length or purity of the pulse. This has been verified by plotting Q values for each source amplitude for

Table VI. Average Q for 0.7-1.0 cps

Explosion	Station	Distance in km	Distance in degree	1 cycle	1 1/2 cycles	Direct Wave
Bilby	Longmire	1178.19	10.59	96.4±18.1	99.6±18.8	
	Hungry Horse	1265.10	11.38	107.7±20.7	124.0±27.3	
	Forsyth	1281.60	11.53	123.9±28.4		
	Tonasket	1335.82	12.02	100.3±16.9		
	Shamrock	1425.80	12.82	135.5±42.7	147.3±22.6	154.5±38.7
	Manhattan	1717.90	15.40	176.8±43.5		
	Durant	1831.00	16.40	137.8±24.7		
	Rolla	2132.80	19.20	176.8±35.2	209.7±49.7	
	Florissant	2256.44	20.30	245.7±66.1		
	St. Louis	2269.15	20.40	211.6±40.9	222.3±52.4	
	Dubuque	2299.25	20.68	193.4±83.9	193.6±40.5	193.6±40.5
	Eutaw	2606.16	23.40	219.6±46.4		
	Cumberland Pl	2727.66	24.50	176.2±28.5		
	Ann Arbor	2819.93	25.30	312.6±91.3		
	Atlanta	2892.20	26.10	388.1±140.4	271.6±68.8	
	Beckley	3056.00	27.48	257.1±68.7		407.8±62.1
	Blacksburg	3146.00	28.30	228.7±43.9		227.4±43.2
	Berlin	3236.00	29.11	273.7±90.2	302.4±71.7	
	State College	3308.78	29.70	380.8±114.9	306.9±79.5	
	LaPalma	3665.05	33.00	296.3±66.6	140.1±14.3	
	Houlton	4066.00	36.56	308.8±61.8		340.2±81.7
	Schefferville	4189.60	37.60	392.5±108.1	428.5±129.3	427.4±42.7
	Resolute	4340.10	38.90	298.6±59.5	297.8±59.1	
	Mould Bay	4372.00	39.20	232.4±35.1	294.2±25.4	
	Alert	5437.97	48.80	417.8±100.6		
	Caracas	5791.92	51.40	461.3±90.3	507.6±143.9	
	Nana	6796.51	61.20	442.4±95.1		
	Kevo	7797.07	70.30	705.4±235.4	898.2±357.8	
	Kiruna	7829.46	70.41	1005.0±478.9	1231.4±394.0	
	Skalstugan	7967.04	71.65	804.7±295.9		
	Sodankyla	8018.26	72.11	559.8±140.3	785.5±240.0	

Table VI. (Continued)

Explosion	Station	Distance in km	Distance in degree	1 cycle	1 1/2 cycles	Direct Wave
Bilby	Umea	8190.71	73.66	646.5±183.8		963.2±172.8
	Konsberg	8198.70	73.73	726.2±204.4	877.6±349.3	
	Kajaani	8361.03	75.19	716.8±232.5	913.1±376.3	
	Goteborg	8452.02	76.01	1145.9±597.3		
	Uppsala	8467.74	76.15	959.1±399.4	1852.1±?	
	Nurmijarvi	8625.57	77.60	659.8±186.0	774.5±474.6	
	Karlskrona	8723.51	78.45	942.7±391.0	1082.2±520.0	
	Bensberg	8803.64	79.20	907.7±353.9	420.5±48.9	
	Matsushiro	8850.53	79.60	1786.8±145.6	4831.6±?	
	Toledo	9029.70	81.21	646.4±172.5	557.9±119.4	
	Pruhonice	9225.16	82.96	662.00±199.2		
	Honiara	10107.07	90.90	587.8±132.1	625.30±150.2	
Gnome	Vernal	1048.27	9.43	133.3		
	Conway	1146.28	10.31	178.3	172.2	
	Jackson	1457.30	13.10	181.4		
	Resolute	4751.56	42.73	331.2	347.0	
	Mould Bay	4965.80	44.66	258.0	312.0	307.0
Haymaker	Rolla	2135.00	19.20	215.1	279.2	265.2
	Madison	2335.00	20.86	236.0	296.0	
	Mould Bay	4371.86	39.31	229.5	205.0	447.7
	Alert	5440.24	48.93	368.1	314.4	
Shoal	Hungry Horse	1075.00	9.67	156.6	315.4	
	Manhattan	1874.45	16.80	165.3	382.6	305.9
	Dallas	2064.17	18.50	384.0	701.0	
	Rolla	2307.99	20.70	409.4	666.4	
	Florissant	2417.73	21.70	385.7	1087.2	
	Oxford	2623.00	23.50	367.4		
	Atlanta	3104.00	27.92	380.4	461.8	
	College Out Post	3436.18	30.90	833.4		

Table VI. (Continued)

Explosion	Station	Distance in km	Distance in degree	1 cycle	1 1/2 cycles	Direct Wave
Shoal	Ogdensberg	3749.10	33.20	507.8	812.1	
	Resolute	4139.61	37.20	287.2	214.0	
	Mould Bay	4131.00	37.20	250.4	293.0	377.9
	Alert	5232.92	47.10	446.9	435.1	
	Arequipa	7849.48	70.50	986.0	1935.3	

various pulse length considerations. The general characteristics of the Q versus epicentral distance envelope for one cycle of the first P arrival may be summarized as seen in Table VII.

Interpretation

Recent evidences concerning the structure and composition of the earth's mantle from the works of various investigators have been summarized by Anderson (1). Existence of a low velocity layer in the upper mantle was advocated by Gutenberg (29) from body wave travel time studies, which was later found to be in agreement with the surface wave dispersion studies by Dorman, Ewing, and Oliver (20) among others. Theoretical studies regarding the inhomogeneities of the upper mantle were made by Birch (11) and Bullen (13, 14). Birch gave a depth range of about 300 to 900 km as an inhomogeneous region which approximately coincides with C region (transition region) of Bullen. Table VIII gives the

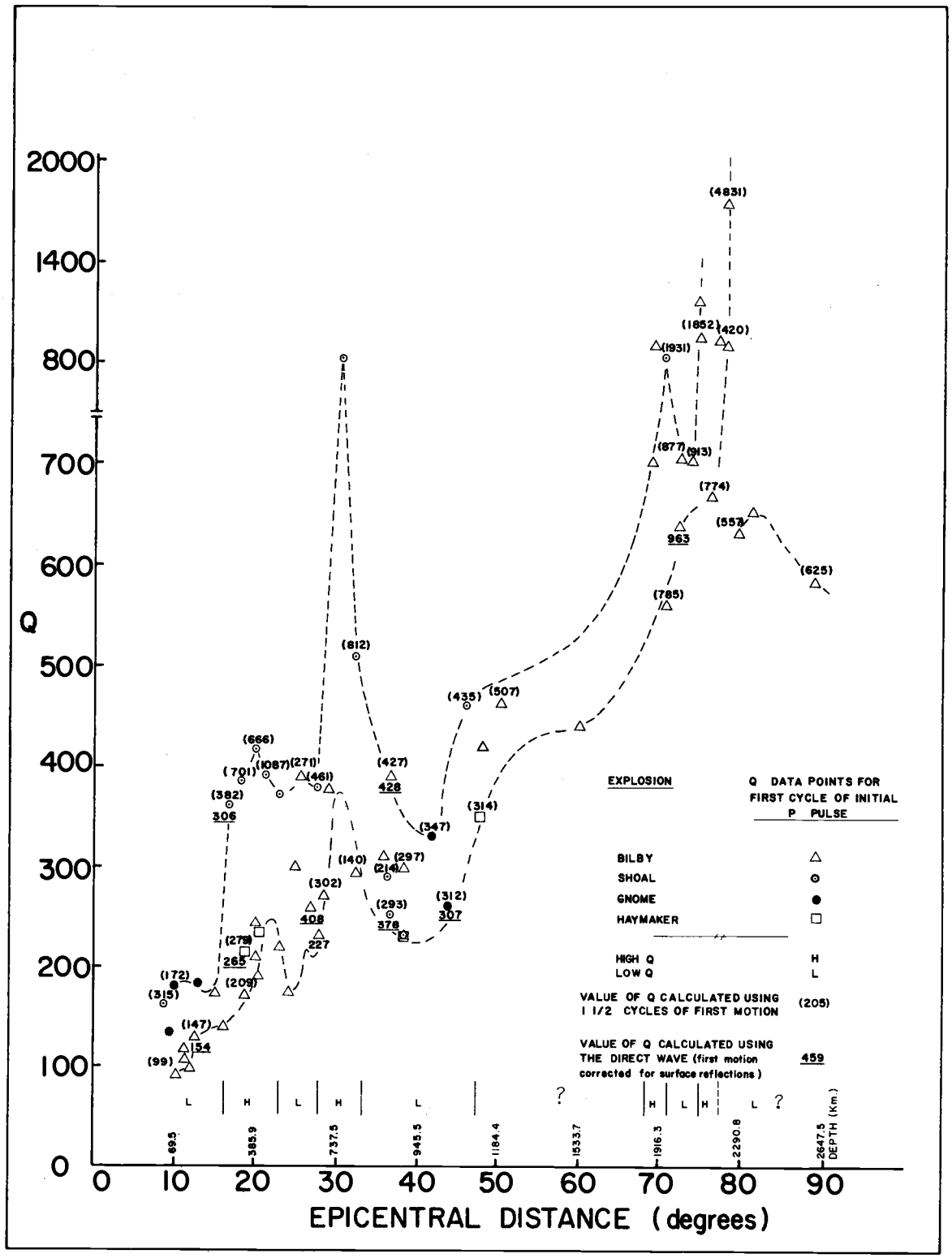

Figure 10. Q versus epicentral distance and depth for first cycle of initial P pulse, 0.7 - 1.0 cps. For comparison Q values for 1 1/2 cycles of first motion and direct waves are shown.

discontinuities in the earth's mantle observed by other investigators. The depths reported here are quoted from the reference cited.

Table VII. General Characteristics of the Q Versus Epicentral Distance Envelope

Epicentral distance in degrees	Maximum depth* of penetration of the rays in km	Feature of the region with respect to Q
9 - 16	57.0 - 185.0	low
16 - 23	185.0 - 575.3	high
23 - 27	575.3 - 695.6	low
27 - 37	695.6 - 905.8	high
37 - 45	905.8 - 1024.2	low
45 - 52	1024.2 - 1227.6	high
52 - 70	1227.6 - 1916.3	questionable because of the lack of data.
70 - 72	1916.3 - 1970.2	high
72 - 75	1970.2 - 2072.6	low
75 - 80	2072.6 - 2290.8	high
80 - 91	2290.8 - 2756.8	low

*The depths reported here were computed using the Herglotz-Wiechert equation (50, p. 669) and Jeffreys-Bullen P wave travel times for surface focus earthquakes.

Only a very rough comparison can be made between Table VII and Table VIII since the depths reported in the latter table were computed by using different travel times by different authors. The discontinuities lying between 190 and 555 km, and at 1140, 1200, 2100 km in depth coincide with regions of high Q, whereas those

between 600 - 700, and at 910, 975 km coincide with regions of low Q. The envelope is questionable for depths between 1200 and 1900 km because of the lack of data.

Table VIII. Discontinuities in the Earth's Mantle

Depth of discontinuity in km	Type observation	Author	Reference
190	P reflections	Hoffman, Berg, and Cook	(30)
200-500 (20° discontinuity)	Travel time	Byerly	(28)
210	P reflections	Hoffman, Berg, and Cook	(30)
225	Travel time and P reflections	Dahm	(19)
350-450	Surface wave dispersion	Töksoz and Anderson	(56)
520	P reflections	Hoffman, Berg, and Cook	(30)
555	P reflections	Hoffman, Berg, and Cook	(30)
600-700	Surface wave dispersion	Töksoz and Anderson	(56)
	Body wave travel time	Nishimura, Kishimoto, and Kamitsuki	(48)
		Doyle and Webb	(21)
910	P reflections	Hoffman, Berg, and Cook	(30)
975 (Repetti's discontinuity)	P reflections	Repetti	(46)
1140	_____	Repetti	(45)
1200	_____	Gutenberg	(45)
1860	_____	Repetti	(45)
1900	_____	Gutenberg	(45)
2100	_____	Repetti	(45)
2150	_____	Gutenberg	(45)

The most peculiar characteristics of the Q vs epicentral distance envelope (see Figure 10) is the presence of low Q, or relatively high absorption, regions superimposed on gradually increasing Q values with epicentral distance. In addition to the high absorption in Gutenberg's low velocity layer--less than 16° epicentral distance--relatively high absorption layers are found to be centered around 25°, 74°, and a broad one at 38° to 47° epicentral distance. Between 52° and 70° there are not enough data to investigate the possibility of a low Q region centered around 61° epicentral distance. The sharp falling off of Q values beyond about 80° as indicated by a few data points between 80° and 91° epicentral distance might indicate the possibility of a high absorption region at about 2350 km in depth.

The reality of the high and low Q regions may be verified from travel time curves. Since the high Q (low absorption) regions might be expected to decrease travel time whereas low Q (high absorption) regions might be expected to increase travel time because of ray path considerations, one could expect that a first or second derivative of a standard travel time curve would indicate these differences if the high absorption regions are actually present in the interior of the earth. The first derivative of the Jeffreys-Bullen P wave travel times for surface focus earthquakes indicates only the 20° discontinuity.

The second derivative of the travel times shows the 20° discontinuity as a very sharp peak. There is considerable scatter in the computed values of the second derivative to an epicentral distance of 80° where the curve becomes smooth. It is possible that maxima and minima corresponding to high and low regions of Q are present, but are masked because of data scatter and a positive correlation can not be made for these data. However, it is possible that when correction of the travel time becomes established well enough, the derivative curves will indicate the regions of high and low Qs.

Discussion

The average of all apparent Q values obtained in this research by using the first cycle of the first arrival P wave is found to be 286 ± 38 for the upper mantle (above 1000 km depth). It is not possible to give the average values of Q for the lower mantle from these data. For rays having a maximum depth of penetration of about 2290 km, computed Q values are very high. The maximum value obtained for this region is above 3000. These values are of the same order of magnitude as those obtained by other investigators (see Table I) and are compatible with those deduced from shear wave data using the argument of Anderson, BenMenahem, and Archambeau.

The general characteristics of the Q vs epicentral distance envelope agree closely with the absorption characteristics observed from surface wave attenuation studies. Anderson and Archambeau's Q distribution models indicate the presence of a broad highly attenuating zone in the upper mantle, a rapid increase in Q at about 400 km in depth and a high Q in the lower mantle. These results agree with those from this study. Knopoff also made a similar observations by using shear waves and indicated the hints of a fine structure for Q in the upper mantle. This is probably reflected in the presence of several peaks and troughs of Q values in the upper mantle (see Figure 10).

The sudden increase in Q values near 20^{o} and subsequent fluctuations superimposed on gradually increasing values up to at least 43^{o} epicentral distance probably indicate the inhomogeneity of the upper mantle proposed by Bullen and Birch from density and elasticity considerations. According to Birch, the inhomogeneous region begins at about 200-300 km in depth. Ferromagnesian silicates gradually shift towards high pressure modifications probably in the form of closely packed oxides below this depth until the transition is completed at a depth of about 800-900 km. If the principal minerals constituting the upper mantle are olivines and pyroxenes, as is commonly believed (51), these minerals should undergo a series of major phase transformations under pressure-temperature conditions corresponding to those between 300 and

900 km. Ringwood (52) has indicated three possible transformations within this depth.

(i) $2MgSiO_3 \longrightarrow Mg_2SiO_4 + SiO_2$

Enstatite (Pyroxene) — fosterite (olivine) — Stishovite

This transformation takes place at pressure-temperature conditions similar to that existing at a depth of 400 km.

(ii) Mg_2SiO_4 (olivine) $\longrightarrow Mg_2SiO_4$ (spinel)

This transformation occurs at 130 ± 20 kb and 600° C which corresponds to a depth of 500-600 km.

(iii) (a) $Mg_2SiO_4 \longrightarrow 2MgO + SiO_2$

Spinel — Periclase — Stishovite

(b) $Mg_2SiO_4 \longrightarrow MgO + MgSiO_3$

Spinel — Periclase — Corrundum

The transformation (a) would occur around 200 kb at 600° C, and for a temperature around 3000° C the required pressure would be about 300 to 350 kb equivalent to a depth of 900 to 1050 km. The density increase due to these transformations in the 300-900 km depth range will be continuous because of the presence of FeO, CaO, Al_2O_3, NiO, Cr_2O_3 and N_2) which will form solid solutions with

the principal magnesium silicate phases. Transformation (b) has been observed experimentally. It is not known whether each peak in the Q vs epicentral distance envelope represents the end of a particular transformation, though the 20° discontinuity has been postulated to be due to the transformation of Olivine to a high pressure form by Bernal and Jeffreys (33). The presence of these low Q regions will then require the materials involved in a transformation to pass through a state in which it will acquire the property of absorbing seismic waves in the frequency range considered in this research, at a temperature and pressure corresponding to the maximum depth of peneteation of the rays yielding low Q values. No such properties have been reported as yet from experiment. However there is experimental evidence of sharp decrease of the dissipation parameter Q for longitudinal waves at the melting point. Laboratory experiments of Mizutani and Kanamori (47) show that there is sharp drop of Q for compressional waves by an order of magnitude at the melting point of an alloy of lead, bismuth, tin and cadmium. No such drops of Q values take place in the upper mantle thereby indicating that the low Q regions might not probably be the regions of melting. However, the sharp decrease of Q values at about 80° epicentral distance amounts to almost an order of magnitude indicating the possibility of melting in that region. Additional experimental work with

different materials might change the speculation.

Because of the lack of data, it is not known whether or not Q decreases from a depth of 2300 km to the core boundary. The observed decrease in Q values between the epicentral distances of 80° and 91°, which correspond to maximum depths of about 2300 and 2700 km respectively, is in contrast with the results previously published by other investigators. Only very recently has decrease of Q towards the core-mantle boundary been reported by Teng (55).

According to Gutenberg and Richter (26) the causes of deep earthquakes are in no essential respect different from those of shallow shocks. However, the maximum number originates within the outer 50 km of the earth (32, p. 34). Though the number diminishes with depth to the limit of 700 km, it shows minima at about 300 km, 450 km, and maxima around 350-400 km and 550-600 km in depth within the limit of accuracy of depth determination. In the Q vs epicentral distance envelope, the depth below the low velocity layer down to 814 km is a region of highly fluctuating Q, below which there is a broad zone of low Q values (high absorption). This zone might not be highly efficient for the accumulation of strain, or the strain accumulation mechanisms might not be highly efficient for producing an earthquake which would be felt at the surface.

Lahiri and Price (38) investigated the induced field and current distributions associated with the magnetic daily and storm time variations by considering electromagnetic induction in a non-uniform sphere. Their results indicated that conductivity increases with depth beyond 250 km, but an important increase takes place at some deeper depth in the upper mantle. The Q versus epicentral distance envelope shows that there is a general increase in Q from about 250 km in depth reaching a maximum value at about 814 km depth in the upper mantle (31^{o} epicentral distance). Thus, the variation of the electric conductivity and absorption properties seems to coincide roughly in this part of the mantle.

CONCLUSIONS

Accurate determination of the apparent value of the dissipation parameter Q requires a thorough knowledge of the (1) displacement pulse used for source amplitude, (2) propagation path, and (3) pulse recorded at teleseismic distance. None of these were thoroughly known in this study. In case (1) the displacement pulses were not simple, and comparisons were made between the observed displacement pulse amplitudes used as source amplitudes and the theoretical source amplitudes for Gnome, Shoal, and Haymaker nuclear explosions. The agreement was good. Since no theoretical source was possible in Bilby, several displacement pulses were considered at different distances for source amplitudes. Q was computed in each case, and an average value was taken as representative of Q for each particular epicentral distance. In case (2), it was travel time and not the path length of propagation that was directly involved in computation, and the Q values were insensitive to small errors in the travel time. In case (3), since the true pulse length was not known at teleseismic distances, computations were made with the

first cycle, and the first one and one half cycles of the recorded first P arrival and the direct wave where possible. Though the absolute values differed somewhat in each computation, especially the higher values, the general trends of variation for different epicentral distances remained the same for all cases.

Within the limitations introduced by the procedure adopted here, the following conclusions may be drawn from the results of this study:

(1) The general trends of variation of the absorptive attenuation properties in the interior of the earth observed from this study are in agreement with the general results obtained from surface wave studies.

(2) There is a general increase in apparent Q values starting at about 16° and continuing to about 80° epicentral distance. The high and low Q regions are superimposed on the gradually increasing Q vs epicentral distance envelope. Thus, it would appear that the mantle of the earth is inhomogeneous with respect to absorption properties to a depth of about 2700 km.

(3) The average apparent Q, using all data of this research for the upper mantle is 286 ± 38.

(4) High Q or relatively low absorption regions are centered around 20°, 31°, 71°, and 78° epicentral distances corresponding to the depth of 385, 786, 1917 and 2233 km, respectively.

(5) Low Q or relatively high absorption regions are centered around 25°, 42°, and 74° epicentral distances corresponding to the maximum depth of 606, 980, and 2072 km, respectively.

(6) Most of the discontinuities in the mantle reported by other investigators from body and surface wave studies coincide reasonably well with the regions of high and low Q.

(7) Maximum depth of earthquake foci is very close to the depth of maximum increase in Q in the upper mantle which is underlain by a broad relatively high absorption region.

(8) Transition from upper to the lower mantle (depth of 1000 km) takes place through a relatively high absorption zone.

(9) The lowest absorption or highest Q region of the mantle obtained in this study occurs in the lower mantle between 2128 and 2291 km in depth (76° - 80° epicentral distance) and not at the lowest part of the mantle considered in this research. There is an indication of an absorption discontinuity at about 80° epicentral distance beyond which a few low Q values have been obtained. The

evidence for this discontinuity is not conclusive as data were available from only three recordings obtained at epicentral distances between 80^{o} and 91^{o}.

BIBLIOGRAPHY

1. Anderson, Don L. Recent evidence concerning the structure and composition of the Earth's mantle. In: Physics and chemistry of the earth, Vol. 6, ed. by L. H. Ahrens, Frank Press, S. K. Runcorn and H. C. Urey. Oxford, London, Pergamon Press, 1965. p. 3-131.

2. Anderson, D. L. and C. B. Archambeau. The anelasticity of the earth. Journal of Geophysical Research 69(10):2071-2084. 1964

3. Anderson, D. L., A. BenMenahem and C. B. Archambeau. Attenuation of seismic energy in the mantle. Journal of Geophysical Research 70(6):1441-1448. 1965.

4. Anderson, D. L. and R. L. Kovach. Attenuation in the mantle and rigidity of the core from multiply reflected core phases. Proceeding of the National Academy of Sciences 51:168-172. 1964.

5. Asada, T. and K. Takano. Attenuation of P waves in the mantle. Journal of Physics of the Earth 11(1):25-34. 1963.

6. Båth, M. and A. Lopez-Arroyo. Attenuation and dispersion of G waves. Journal of Geophysical Research 67(5):1933-1942. 1962.

7. BenMenahem, A. Observed attenuation and Q values of seismic surface waves. Journal of Geophysical Research 70(18):4641-4651. 1965.

8. Berg, J. W., Jr. and G. E. Papageorge. Elastic displacement of primary waves from explosive sources. Bulletin of the Seismological Society of America 54(3):947-960. 1964.

9. Berg, J. W., Jr., L. D. Trembly and P. R. Laun. Primary ground displacements and seismic energy near Gnome Explosion. Bulletin of the Seismological Society of America 54(4):1115-1126. 1964.

10. Birch, F. Hand book of physical constants. New York, 1942. 325 p. (Geological Society of America. Special paper no. 36)

11. Birch, F. Elasticity and constitution of the earth's interior. Journal of Geophysical Research 57(2):227-286. 1952.

12. Born, W. T. The attenuation constants of the earth materials. Geophysics 6(2):132-148. 1941.

13. Bullen, K. E. The variation of densities and elasticities of strata of equal density within the earth. Monthly Notices of Royal Astronomical Society (Geophysical supplement) 3:395-401. 1936.

14. _____. The problem of earth's density variations. Bulletin of the Seismological Society of America 30(1):235-250. 1940.

15. _____. Theoretical Seismology. Cambridge, At the university Press, 1963. 381 p.

16. Carder, D. S. Ground effects from the Gnome and Logan explosions. Bulletin of the Seismological Society of America 52(5):1047-1056. 1962.

17. Carpenter, E. W. Teleseismic methods for the detection, identification, and location of the underground explosions. Ann Arbor, University of Michigan, Institute of Science and Technology, Acoustic and Seismic Laboratory, 1964. 27 p. (VESIAC State-of-the-Art Report. Contract SD-78).

18. Collins, F. and C. C. Lee. Seismic wave attenuation characteristics from pulse experiments. Geophysics 21(1):16-39. 1956.

19. Dahm, C. G. Velocities of P and S waves calculated from the observed travel times of the Long Beach earthquake. Bulletin of the Seismological Society of America 26(1):159-171. 1936.

20. Dorman, James, Maurice Ewing and Jack Oliver. Study of shear velocity distribution in the upper mantle by mantle Rayleigh waves. Bulletin of the Seismological Society of America 50(1):87-115. 1960.

21. Doyle, H. A. and J. P. Webb. Travel times to Australian stations from Pacific nuclear explosions in 1958. Journal of Geophysical Research 68(4):115-1120. 1963.

22. Ewing, M. and Frank Press. An investigation of the mantle Rayleigh waves. Bulletin of the Seismological Society of America 44(2A):127-147. 1954.

23. Futterman, W. I. Dispersive body waves. Journal of Geophysical Research 67(13):5279-5291 1962.

24. Gutenberg, B. Amplitude of surface waves and magnitude of shallow earthquakes. Bulletin of the Seismological Society of America 35(1):3-12. 1945.

25. _____. Amplitude of P, PP and S, and magnitude of shallow earthquakes. Bulletin of the Seismological Society of America 35(1):57-69. 1945.

26. Gutenberg, B. and C. F. Richter. Evidence from deep focus earthquakes. In: Internal constitution of the earth, ed. by B. Gutenberg. 2d ed. New York Dover Publications, 1951. p. 305-313.

27. Gutenberg, B. Attenuation of seismic waves in the earth's mantle. Bulletin of the Seismological Society of America 48(3):269-282. 1958.

28. _____. Physics of the earth's interior. New York, Academic Press, 1959. 240 p.

29. _____. Wave velocities below the Mohorovicic discontinuity. Geophysical Journal 4:348-352. 1959.

30. Hoffman, John P, Joseph W. Berg, Jr. and Kenneth L. Cook. Discontinuities in the earth's upper mantle as indicated by reflected seismic energy. Bulletin of the Seismological Society of America 51(1):17-27. 1961.

31. Howell, B. F., Jr. Absorption of seismic waves. Ann Arbor, University of Michigan, Institute of Science and Technology, Acoustic and Seismic Laboratory, 1963. 27 p. (VESIAC State-of-the-Art Report. Contract SD-78)

32. Jacobs, J. A., R. D. Russell and J. T. Wilson. Physics and geology. New York, McGraw-Hill, 1959. 424 p.

33. Jeffreys, H. The earth. 3d ed. Cambridge, At the University Press, 1952. 392 p.

34. Jeffreys, H. and K. E. Bullen. Seismological tables. London, Office of the British Association, Burlington House, W. R. 1940. p. 50.

35. Knopoff, L. Q. Reviews of Geophysics 2(4):625-660. 1964.

36. Knopoff, L. and G. J. F. MacDonald. Attenuation of small amplitude stress waves in solids. Reviews of Modern Physics 30(4):1178-1192. 1958.

37. Kovach, R. L. and D. L. Anderson. Attenuation of seismic waves in the upper and lower mantle. Bulletin of the Seismological Society of America 54(6):1855-1864. 1964.

38. Lahiri, B. N. and A. T. Price. Electromagnetic induction in non-uniform conductors, and the determination of the electrical conductivities of the earth from terrestrial magnetic variations. Royal Society of London Proceedings, Ser. A, 165:S55-S56. 1938.

39. Lamb, G. L., Jr. The attenuation of waves in a dispersive medium. Journal of Geophysical Research 67(13):5273-5278. 1962.

40. Lomnitz, C. Linear dissipation in solids. Journal of Applied Physics 28(2):201-205. 1957.

41. Long Range Seismic Measurements, Project 8.4, "Haymaker" prepared for AFTAC, Washington, D. C. under ARPA project: VELA-UNIFORM, 7 October, 1962. Garland, Texas.

42. Long Range Seismic measurements. Project 8.4 "BILBY" prepared for AFTAC, Washington, D. C. under ARPA project: VELA-UNIFORM, 8 November, 1963. Alexandria, Va. (Contract AF 33(657)-12447. VT/2037. DATDC report no. 87)

43. Long Range Seismic Measurements. Project 8.4 "Shoal" prepared for AFTAC, Washington D. C., Under ARPA project: VELA-UNIFORM 9 December, 1963. Alexandria, Va. (Contract AF 33(657)-12447. VT/2037. DATCD report no. 92)

44. MacDonald, J. R. Rayleigh wave dissipation function in low loss media. Geophysical Journal 2(2):132-135. 1959.

45. Macelwane, J. B. Evidence on the interior of the earth derived from seismic sources. In: Internal constitution of the earth, ed. by B. Gutenberg. New York, Dover, 1951. p. 227-304.

46. Macelwane, J. B. and F. W. Sohon. Introduction to theoretical seismology. St. Louis, St. Louis University. 1932. 366 p.

47. Mizutani, H. and H. Kanamori. Variation of elastic wave velocity and attenuation property near the melting temperature. Journal of Physics of the Earth 12(2):43-49. 1964.

48. Nishimura, E., Y. Kishimoto and A. Kamitsuki. On the nature of 20° discontinuity in the Earth's mantle. Tellus 10(1):137-144. 1958.

49. Press, F. Rigidity of the earth's core. Science 124:1204. 1956.

50. Richter, C. F. Elementary seismology. San Francisco, W. H. Freeman, 1958. 768 p.

51. Ringwood, A. E. Mineral constitution of the deep mantle. Journal of Geophysical Research 67)10):4005-4010. 1962.

52. _____. Phase transformations in the mantle. In: Nuclear Geophysics. Washington, D. C., 1963. p. 19-24. (National Research Council. Publication no. 1075)

53. Romney, Carl, B. G. Brooks, R. H. Mansfield, D. S. Carder, J. N. Jordan and D. W. Gordon. Travel times and amplitudes of principal body phases recorded from Gnome. Bulletin of the Seismological Society of America 52(5):1057-1074. 1962.

54. Sato, Y. Attenuation, dispersion, and wave guide of G wave. Bulletin of the Seismological Society of America 48(3):231-251. 1958.

55. Teng, Ta-Liang. P wave attenuation in the mantle. (Abstract). American Geophysical Union Transactions 47(1):162-163. 1966.

56. Töksoz, N. and D. L. Anderson. Phase velocities of long period surface waves and the structure of the upper mantle. 1. Great circle Love and Rayleigh wave data. Journal of Geophysical Research 71(6):1649-1658. 1966.

57. Trembly, L. D. and J. W. Berg, Jr. Amplitudes and energies of primary seismic waves near the Hardhat, Shoal and Haymaker explosions. Bulletin of the Seismological Society of America 56(3):643-653. 1966.

58. Wegel, R. L. and H. Walther. Internal dissipation in solids for small cyclic strains. Physics 6(4):141-157. 1935.

59. Werth, G. C., R. F. Herbst and D. L. Springer. Amplitude of the seismic arrivals from M discontinuity. Journal of Geophysical Research 67(4):1587-1610. 1962.

60. Yamakawa, N. and Y. Sato. Q of the surface waves. Journal of Physics of the Earth 12(1):5-18. 1964.

61. Zemanek, Joseph, Jr. and Isadore Rudnick. Attenuation and dispersion of elastic waves in a cylindrical bar. Journal of the Acoustical Society of America 33(10):1283-1288. 1961.

APPENDICES

APPENDIX I

SEISMOGRAPH STATION LOCATIONS, CO-ORDINATES, TYPES OF INSTRUMENTS USED AND THE EVENTS RECORDED

Seismograph Stations

Location	Abbreviation	Event* recorded	Type of instrument	Latitude	Longitude
Alert, Canada	ALE	H, S, B	Willmore	82°29'00.0"N	62°24'00.0"W
Ann Arbor, Michigan	AAM	B	Benioff	42°17'59.0"N	83°39'22.0"W
Arequipa, Peru	ARE	S	"	16°27'43.5"S	71°29'28.6"W
Atlanta, Georgia	ATL	B	"	33°26'00.0"N	84°20'15.0"W
Beckley, West Virginia	BLWV	B	"	37°47'56.0"N	81°18'36.0"W
Bensberg, Germany	BNS	B	Hiller	50°57'50.0"N	7°10'32.0"E
Berlin, Pennsylvania	BRPA	B	Benioff	39°55'22.0"N	78°50'33.0"W
Blackesberg, Virginia	BLA	B	"	37°12'40.0"N	80°25'14.0"W
Caracas, Venezuela	CAR	B	"	10°30'24.0"N	66°55'39.5"W
College Out post, Alaska	COL	S	"	64°54'00.0"N	147°47'36.0"
Conway, Arkansas	CWAR	G	"	35°08'08.0"N	91°58'40.0"W
Cumberland Pl, Tennessee	CPO	B	spJ. M	35°35'41.4"N	85°34'13.5"W
Dallas, Texas	DAL	S	Benioff	32°50'46.0"N	96°47'02.0"W
Dubuque, Iowa	DBQ	B	"	42°30'24"N	90°41'00.0"W
Durant, Oklahoma	DUOK	B	"	34°02'11.0"N	96°13'04.0"W
Eutaw, Alabama	EUAL	B	"	32°47'10.0"N	87°52'00.0"W
Florissant, Missouri	FLO	B	"	38°48'06.0"N	90°22'12.0"W
Forsyth, Montana	FRMA	B	"	46°06'00.0"N	106°26'25.0"W
Goteborg, Sweden	GOT	B	Grenet	57°41'54.0"N	11°58'47.0"E
Honiara, Solomon Isl	HNR	B	Benioff	9°25'53.9"S	159°56'47.6"E
Houlton, Main	HNME	B	"	46°09'43.0"N	67°59'09.0"W
Hungry Horse, Montana	HHM	S, B	"	48°20'58.0"N	114°01'39.0"W
Jackson, Tennessee	JSTN	G	"	35°39'20.0"N	88°36'46.0"W
Kajaani, Finland	KJN	B	"	64°05'07.0"N	27°42'43.0"E
Karlskrona, Sweden	KLS	B	Grenet	69°45'24.0"N	15°35'30.0"E
Kevo, Sweden	KEV	B	Benioff	69°45'24.0"N	27°00'54.0"E
Kiruna, Sweden	KIR	B	Grenet	67°50'24.0"N	20°25'00.0"E
Konsberg, Norway	KON	B	Benioff	59°40'00.0"N	09°40'00.0"E
LaPalma, El Salvador	LPS	B	"	14°17'32.0"N	89°09'43.0"W
Longmire, Washington	LON	B	"	46°45'00.0"N	121°48'36.0"W

Seismograph Stations (Continued)

Location	Abbreviation	Event recorded	Type of instrument	Latitude	Longitude
Madison, Wisconsin	MDS	H	Benioff	43°22'20.0"N	89°45'36.0"W
Manhattan, Kansas	MHT	S, B	"	39°11'59.0"N	96°34'50.0"W
Matsushiro, Japan	MAT	B	Short period	36°32'30.0"N	138°12'32.0"E
Mould Bay, Canada	MBC	G, S, H, B	Willmore	76°14'00.0"N	119°20'00.0"W
Nana, Peru	NNA	B	Benioff	11°59'15.2"S	76°50'31.7"W
Nurmijarvi, Finland	NUR	B	"	60°30'32.2"N	24°39'18.1"E
Ogdensberg, New Jersey	OGD	B	"	41°04'00.0"N	74°37'00.0"W
Oxford, Mississippi	OXF	B	"	51°46'00.0"N	01°15'00.0"W
Pruhonice, Czechoslovakia	PRU	B	SVSN-4	49°59'18.0"N	14°32'30.0"E
Resolute, Canada	RES	G, S, B	Willmore	74°41'12.0"N	94°54'00.0"W
Rolla, Missouri	ROL	S, H, B	Benioff	37°55'04.0"N	91°52'08.0"W
Schefferville, Canada	SCH	B	Willmore	54°49'00.0"N	66°47'00.0"W
Shamrock, Texas	SKTX		Benioff	35°04'58.0"N	100°21'50.0"W
Skalstugan, Sweden	SKA	B	Grenet	63°34'48.0"N	12°16'48.0"E
Sodankyla, Finland	SOD	B	Benioff	67°22'16.2"N	26°37'44.7"E
St. Louis, Missouri	SLM	B	"	38°38'10.0"N	90°14'10.0"W
State College, Pennsylvania	SCP	B	"	48°48'35.5"N	77°52'09.8"W
Toledo, Spain	TOL	B	"	39°52'53.0"N	04°02'55.0"W
Tonasket	TKWA		"	48°47'38.0"N	119°35'16.0"W
Umea, Sweden	UME	B	"	63°48'54.0"N	20°14'12.0"E
Uppsala, Sweden	UPP	B	"	59°51'29.0"N	17°37'37.0"E
Vernal, Utah	VNUT		"	40°30'31.0"N	109°34'45.0"W

* B = Bilby H = Haymaker G = Gnome S = Shoal

APPENDIX II

DIAGRAMS OF THE DISPLACEMENT PULSES USED FOR THE COMPUTATIONS OF THE SOURCE AMPLITUDE

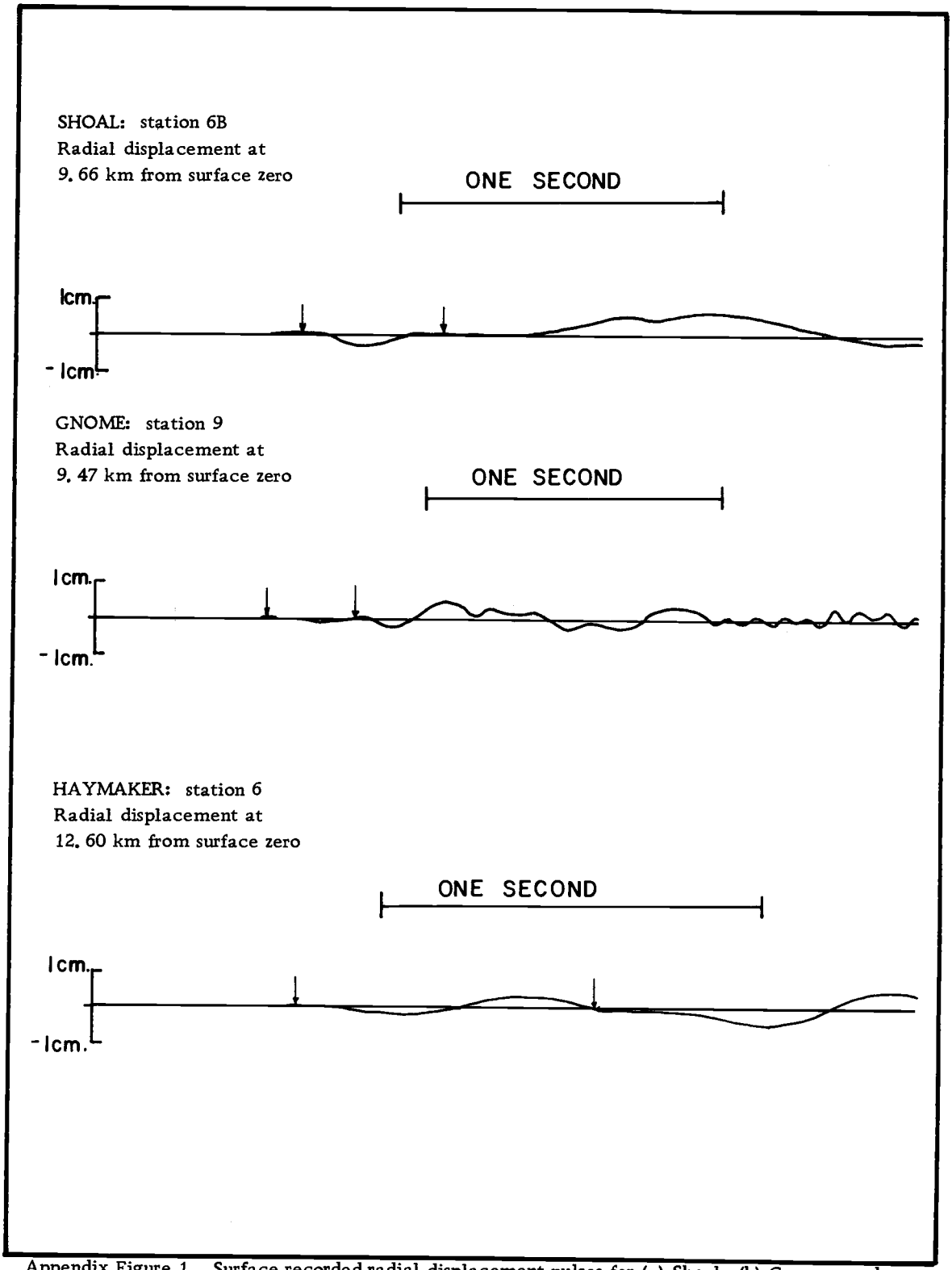

Appendix Figure 1. Surface recorded radial displacement pulses for (a) Shoal, (b) Gnome, and (c) Haymaker underground nuclear explosions used for computation of source amplitudes. The pulse length between the two arrows were used for amplitude computations.

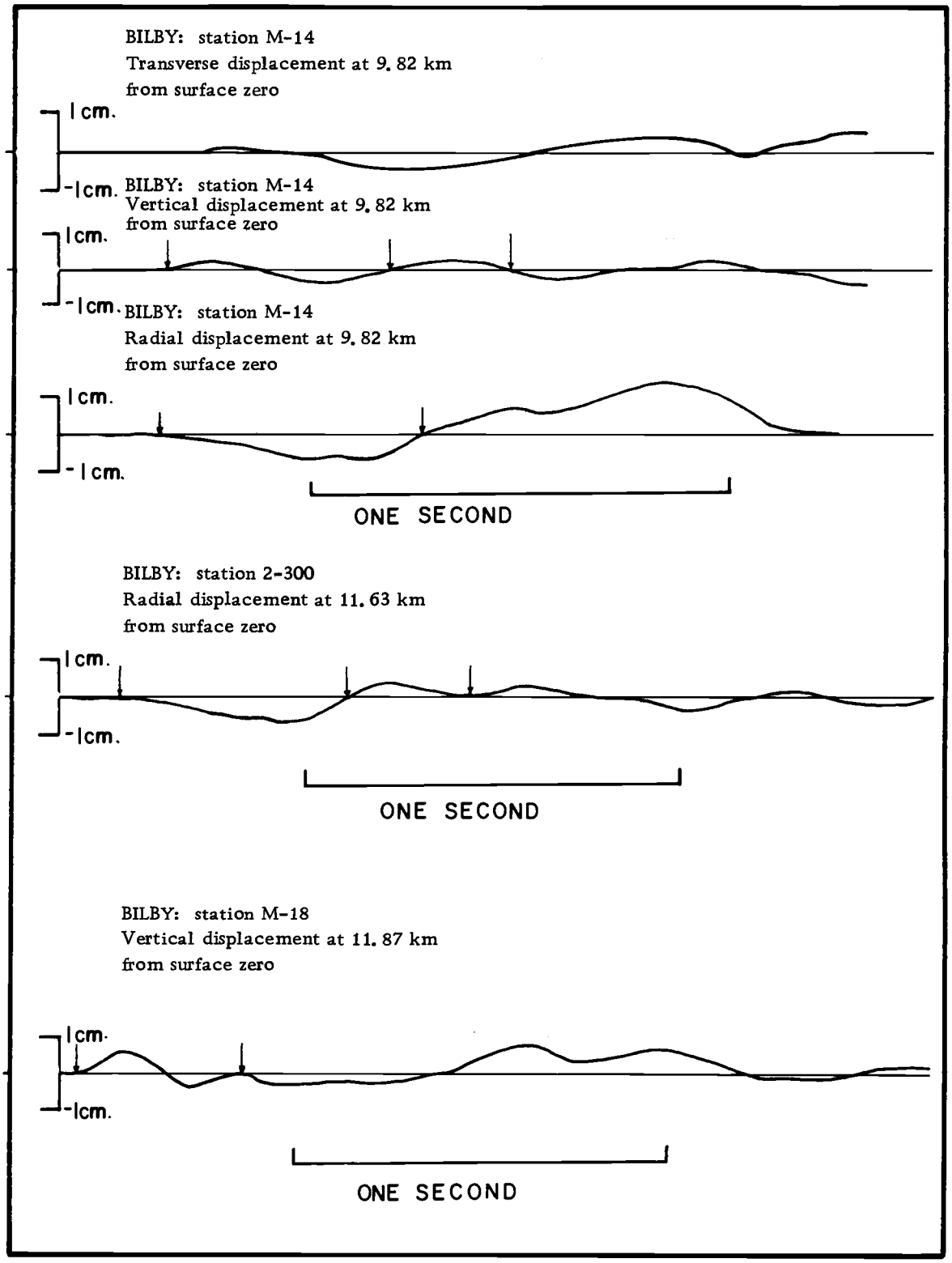

Appendix Figure 2. Surface recorded displacement pulses for Bilby underground nuclear explosion used for computations of source amplitude. The pulse length between the first arrow and any one of the next was used for computation of source amplitude.

APPENDIX III

SEPARATION OF PULSES

SEPARATION OF SURFACE REFLECTION FROM P PULSE RECORDED AT TELESEISMIC DISTANCES

If there is reflection of the compressional wave at the free surface resulting from an underground nuclear explosion, the reflected wave will follow very nearly the same path as the direct wave. In that case, the first P wave arrival recorded at teleseismic distances will be a resultant of the superposition of direct and reflected waves--the reflected wave being delayed by a time interval which is approximately equal to twice the time necessary for the compressional wave to travel from the shot point to the free surface. The amplitude of the reflected wave will vary depending upon the epicentral distance because the angle of incidence of the reflection at the free surface will change as a function of recording distance.

If the wave forms of the direct and reflected waves are identical except for a 180° phase difference, the first part of the recorded wave form of P will be pure to a time equal to the delay time of the reflected wave and the direct and reflected waves can be separated by progressive addition.[1]

---

[1] This method was also suggested by Carpenter (1964) (17).

If: $A(t)$ = the amplitude of the recorded wave at time 't' from the onset;

$a(t)$ = the amplitude of the direct wave at time 't' from the onset;

λ = the delay time of the reflected arrival; and

e = a fraction ≤ 1,

Then:

$$A(t) + ea\,(t-\lambda) = a(t) \qquad (1)$$

where $a\,(t-\lambda) = 0$ when $(t-\lambda) < 0$

For example:

$A_1, A_2, A_3 \ldots\ldots A$ are successive digitized amplitude values of the recorded pulse.

$a_1, a_2, a_3 \ldots\ldots A$ are successive digitized amplitude values of the pure direct wave.

If the delay time, λ, is selected by trial and error, such that A_{15} is the first digitized amplitude value contaminated by the surface reflection and e is one, $A_{15} + a_1 = a_{15}$. Since $A_1 = a_1$, $A_2 = a_2$, $A_3 = a_3 \ldots\ldots$, $A_{14} = a_{14}$, the pure pulse amplitude at the next time interval has been obtained by equation (1). The process can be continued until the surface reflection has been separated.

In practice, different values of λ must be assumed and the

process tried until separation occurs at the correct values of λ and e. Also, the pure pulses usually cannot be separated entirely because another arrival generally occurs within one second after the onset time of the first arrival. In the cases tried, the digitizing interval was 0.02 sec. λ was first assumed to be 0.2 seconds and was increased by 0.02 seconds after each trial until separation occurred.

A few examples of this pulse separation are given in Figure 3 which shows the separation of three pulses from the original P pulse recorded at Mould Bay from the Gnome, Shoal, and Haymaker nuclear explosions. The amplitude of the reflected wave was assumed equal to that of the direct wave in each case. Appendix Table 1 gives the results of this analysis.

Appendix Table 1. Examples of Separation of Surface Reflections from P Pulse Recorded at Mould Bay (Times of Arrival of Pulses Resulting from Separation are Given in Seconds after the First Onset)

Explosion	Time of Arrival of 1st Dilatational Pulse from Separation (Sec. after 1st Arrival)	Time of Arrival of Second Compressional Pulse from Separation (Sec. after 1st Arrival)
Gnome	0.3	0.6-0.7
Haymaker	0.5	0.8
Shoal	0.3	0.6

Dr. W. D. Weart (personal communication) gave the following arrival times from the close-in measurement data:

Appendix Table II. Time of Arrival of Pulses from Close-in Measurements

Event	Instrument Location (Feet from Surface Zero)	Time of Arrival of Pulses (Seconds after 1st Arrival)
Gnome	0	0.16 1.16 1.68 1.99
Haymaker	650	0.29 0.73
Shoal	0	0.09 0.78

The times of arrivals of the surface reflected wave in Mould Bay records come very close to those measured in the close-range. The other values do not seem to agree for Gnome, but there may be correspondence for records from Haymaker and Shoal with the close-range data.

This procedure does not give separation when applied to the records which show the wave form of the first arrival having the third half cycle (of the first arrival) amplitude much smaller than that of second half cycle or deformed by new arrivals.

It should be pointed out that it has not been established that this method gives a unique separation of the pulses.

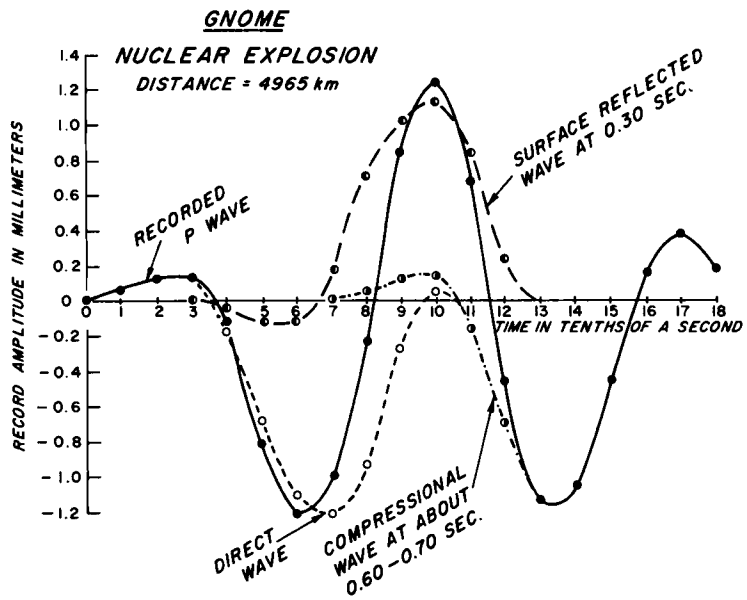

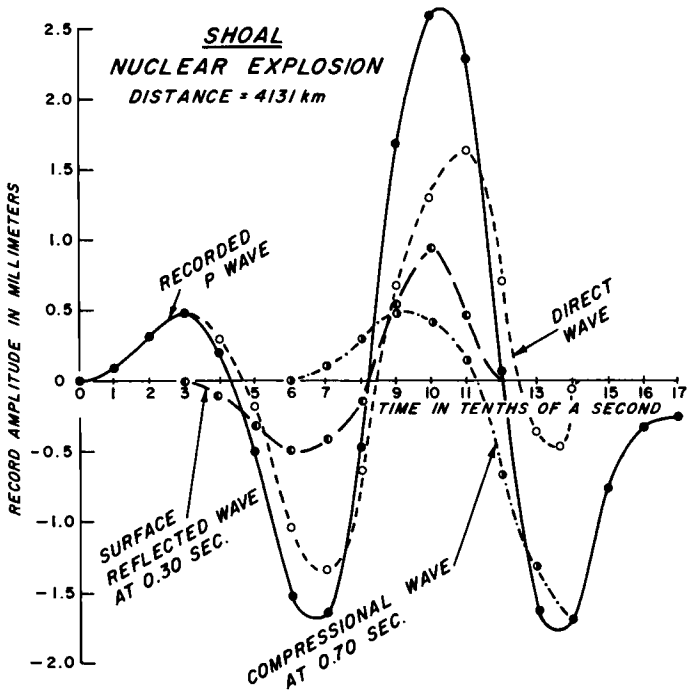

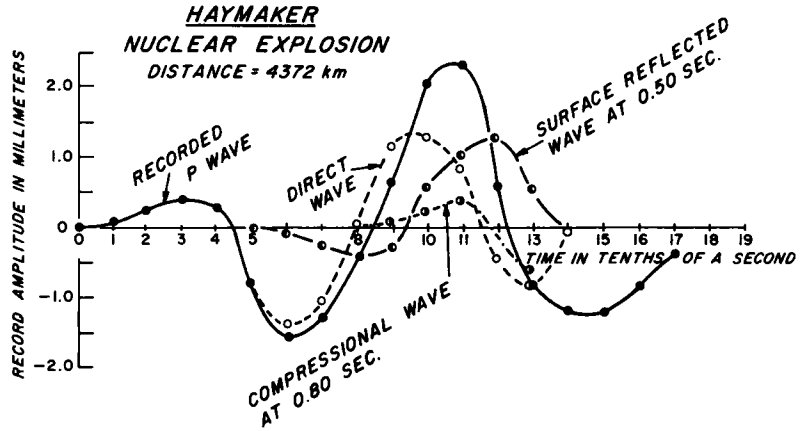

Appendix Figure 3.

Examples of separation of pulses from the original P pulse (first arrival) recorded at Mould Bay from Gnome, Shoal, and Haymaker underground nuclear explosions.